The use of chain extenders as processing aids in the valorization of single-use polylactide (PLA) products by rotomolding

Mateusz Barczewski[1*], Joanna Aniśko[1], Aleksander Hejna[1], Mariusz Marć[2], Marta Safandowska[3], Krzysztof Lewandowski[4], Zaida Ortega[5], Patryk Mietliński[6], Jacek Andrzejewski[1]

Abstract

Biodegradable plastics in single-use products have increased popularity as a way to reduce the negative environmental impact of conventional plastics. However, their recyclability needs to be assessed, as the environmental behavior of single-use plastics, even if compostable, is not negligible. Polylactide (PLA) is susceptible to thermal, oxidative, hydrolytic, and mechanical degradation during reprocessing, so the conditions of such cycles must be accurately controlled. The necessity of using additives to reduce such degradations during rotational molding, a process with long cycle times and oxidizing atmosphere, has been demonstrated. Chain extenders based on a carbodiimide (Bioadimide® 100), a diisocyanate (MDI), and a polystyrene-acrylic copolymer (Joncryl®) have been added to post-consumer PLA wastes. It has been demonstrated that the three chain extenders used allow for obtaining a higher molecular weight of the polymer after the reprocessing, compared to the reduction of about half in molecular weight for the neat PLA after reprocessing, the use of carbodiimide leading to obtain materials with properties most similar to the unprocessed raw material. All samples provided adequate thermal stability and processing parameters for rotomolding. Carbodiimide is considered the most efficient additive, as it increases the molecular weight of the polymer and also its stability, as it remains ~~while keeping it~~ unchanged after the rotomolding process. Similarly, rheological behavior remains unchanged ~~before and~~ after processing, which means that this compound can reduce thermooxidative and hydrolytic degradation reactions, thus contributing to the achievement of an improved processability and better performance; in particular, impact strength increased from 1.06 ± 0.56 for PLA to 8.12 ± 2.28 kJ/m^2 for PLA-KI, and toughness of 5.36 ± 1.61 to 61.49 ± 8.01 J/mm^3, respectively, leading to rotomolded items without structural defects. On the opposite, the use of Joncryl® and MDI led to structural defects in the rotomolded parts, despite also contributing to a higher molecular weight of the polymer, which resulted in poor mechanical properties, although better than PLA without any additive. All three chain extenders resulted in an amorphous material with increased glass transition temperature and improved thermal stability, which correlated with the reduced emissions of volatile compounds, compared to neat recycled PLA. These findings contribute to a better understanding of PLA and its modifications at a molecular scale due to its reprocessing, knowledge which is crucial for optimizing its environmental performance and widening its applications, particularly in a process with long cycle times and oxidative character, such as rotomolding.

Keywords: PLA, waste valorization, waste management, rotational molding, chain extenders, stabilization

1. Introduction

Rotational molding or rotomolding is a technology that allows forming of thin-wall products, including large-size ones, in a one-stage process. The process consists in introducing a polymeric powder into a closed mold representing the outer surface of the part, putting this mold in motion in two axes while heating it, gradually sinters and then completely melts on the inner surface of the mold. After this, the cooling stage starts, ending the cycle with the product demolding [1,2]. The most often used material is polyethylene (PE), mainly high-density or linear low-density grades [3]. This polymer is characterized by good thermal and thermo-oxidative stability, which allows the shaping process to be carried out under the long-term thermal stress of the molded material in an oxidizing atmosphere. There are currently many attempts to make the rotomolding process more sustainable, and pulverized recycled materials are more commonly being used. Different published studies have assessed the use of polymers derived from recycling [4–6] and the introduction of renewable [7–9] or post-consumer, post-production [10,11] materials. However, no research on the use of chain extenders or stabilizers on recycled polymers have been performed for rotational molding products to date.

The increasing polylactide (PLA) share in the packaging materials market causes additional risks related to its subsequent management. While post-consumer PLA products can be utilized in industrial composting processes, using a biodegradable polymer characterized by a high price as a single-use material raises many concerns from the energy balance perspective in relation to the assumptions of the Circular Economy [12]. Many researchers have described mechanical recycling and the impact of multiple processing and process conditions during melt-processing on PLA in detail [13–17]. For instance, Badia and Ribes-Greus [14] emphasized the critical role of the use of multi-criteria evaluation of mechanical recycling processes, allowing for a comprehensive approach to the susceptibility of materials for further applications. The complex analytical system should consist of: i) reprocessing and service life simulation; ii) structural assessment; iii) morphological, rheological, thermal, and mechanical characterization; iv) monitoring low-molecular weight compounds; and v) application-driven characterization. This approach is essential in the case of the implementation of new processing technologies and methods of stabilizing biodegradable polyesters. Żenkiewicz et al. [15] studied the influence of multiple extrusion processes as a laboratory-conducted analysis of the susceptibility of PLA to mechanical recycling. These authors showed that 10-times processing caused only a 6 % decrease in tensile strength (68 MPa after ten processing cycles vs. 72 MPa for the virgin material) and a slight reduction in impact strength from 2.5 to 2 kJ/m^2. It should be emphasized that obtaining such small changes in properties caused by multiple processing is impossible in industrial conditions due to the higher process efficiency, which translates into the intensification of degrading factors such as melt temperature and shear forces. Another problem of PLA mechanical recycling was considered by Beltran and co-workers [18,19], who studied the impact of an additional water bath cleaning procedure on inter-process polylactide in food processing applications. It was shown that the implementation of washing steps decreased the intrinsic viscosity ~~(IV)~~ by 16% compared to virgin PLA, which was associated with the effects of hydrolytic degradation during melt processing. It should be underlined that all studies related to mechanical recycling are conducted by manufacturing methods with high process efficiency (extrusion and injection molding) [13], in which the thermal load under oxidative conditions lasts relatively short, contrarily to what happens in rotational molding. As shown by Cuadri et al. [20], thermoooxidative and thermomechanical are the dominant forms of degradation during

the melt-processing of PLA in those technologies. Contrarily, for rotational molding, the degradation is mainly aatributed to thermooxidative phenomena, due to the lack of shear forces. The problem of stabilization of PLA in rotational molding has not been described in the literature to date, which constitutes one of the novelties of the work presented. Our previous work [21] showed that it is possible to valorize post-consumer PLA waste from disposable cups using rotational molding technology. Apart of conducting a preprocessing to increase the material crystallinity (annealing) and reduce the degradation effects due to the long-term exposure to relatively high temperatures under oxidizing conditions typical of rotomolding, that research ~~clearly showed~~ demonstrated the need for additional chemical stabilization of the PLA structure before being subjected to the rotational molding process, especially when intending to use reclaimed material.

During melt processing, thermal, thermooxidative, thermomechanical, and hydrolytic degradation occurs mostly simultaneously; therefore, it is difficult to separate those processes and tailor the chain extender or stabilizer with a suitable structure. During thermal degradation, unzipping depolymerization and random main chain scission reactions occur, while in the case of hydrolysis and oxidative degradation ~~scission~~ reactions, cis-elimination and intra- and intermolecular transesterification processes are usually noted [22,23]. All those processes may be limited by joining polymer active chain-end groups using chain extenders (CE). CEs are introduced as reactive components with a polymer chain to improve their compatibility in a mixture with other polymers (PBAT, PCL, PA11, POM) [24–28], reducing the negative impact of processing conditions [29] or susceptibility to hydrolytic degradation [30]. In former studies, various modifiers were used as CE for stabilizing the PLA, including poly(styrene-acrylic-co-methacrylate glycidyl) copolymers (Joncryl®) [27,31,32], polycarbodiimides (PCDI) [31,33], isocyanates (MDI, PAPI, HDI) [34–36], tris(nonylphenyl)phosphate (TNPP) [31,37], and ~~the composition of~~ an epoxydized soybean oil (ESO) with dicarboxylic acids (DCAs) [38,39]. Due to the chemical structure of PLA, the mechanisms of interaction of various CEs will involve the attachment of their functional groups ~~contained in them~~ to the hydroxyl (-OH) and carboxyl (-COOH) groups located on the backbone of the polymer chain [31]. The most commonly used compounds contain epoxy groups, as Joncryl® or epoxidized oils, which reacts with both hydroxyl and carboxyl groups in PLA at the chain ends [19,40]. It should be emphasized, however, that the reaction with electrophilic epoxide groups is more easily conducted with carboxyl groups in polyesters [31,41]. The introduction of polycarbodiimide to the structure of PLA is also associated with the reaction of -N=C=N- bonds with -COOH or -OH groups of PLA [33]. When diisocyanates are used, a reaction of the -N=C=O groups with the hydroxyl groups occurs, leading to the formation of urethane bonds or with carboxylic end groups of PLA forming amide linkage [35].

The acting mechanisms ~~of deposition~~ of these CEs are well described in the literature, although it should be emphasized that most works focus on increasing the thermal resistance of the modified polymer. Experiments have been carried out so far have assessed ~~on~~ the long-term effects of temperature and oxidizing atmosphere [20]. However, these were only single rheological experiments performed under steady shearing conditions to elucidate the mechanisms involved in degradation and did not involve processing under real conditions. The aim of this research work, namely the assessment of chain extenders to improve the processability and the performance of recycled PLA fractions in rotational molding, has not yet

been envisaged in the literature. No attempts have been described in the literature to use any of the CEs mentioned above to enhance the stability of PLA in terms of the demanding rotational molding process. Therefore, the main innovation presented in this research is the valorization of post-consumer waste from thermoformed disposable polylactide vessels as a raw material for rotomolding.

2. Experimental

2.1. Materials ~~and sample preparation~~

Post-consumer polylactide (PLA) obtained from the fragmentation of disposable cups with a capacity of 0.5 dm^3 (PAPSTAR Kall, Germany) was used for the research. The material before reprocessing had a melt flow index (MFI) of 15.1 ± 1.3 g/10 min (210 °C; 2.16 kg). Our previous work described the characterization and processing of this PLA waste in detail [21].
Three compounds were used as PLA chain extenders: poly(styrene-acrylic-co-methacrylate glycidyl) copolymer Joncryl® ADR-4368c (BASF) (J), bis(2,6-diisopropylphenyl)carbodiimide Bioadimide® 100 (Lanxess) (KI), and 4,4'-methylenediphenyl diisocyanate (MDI) (Sigma Aldrich). The chemical formulae of the modifiers are presented in Figure 1.

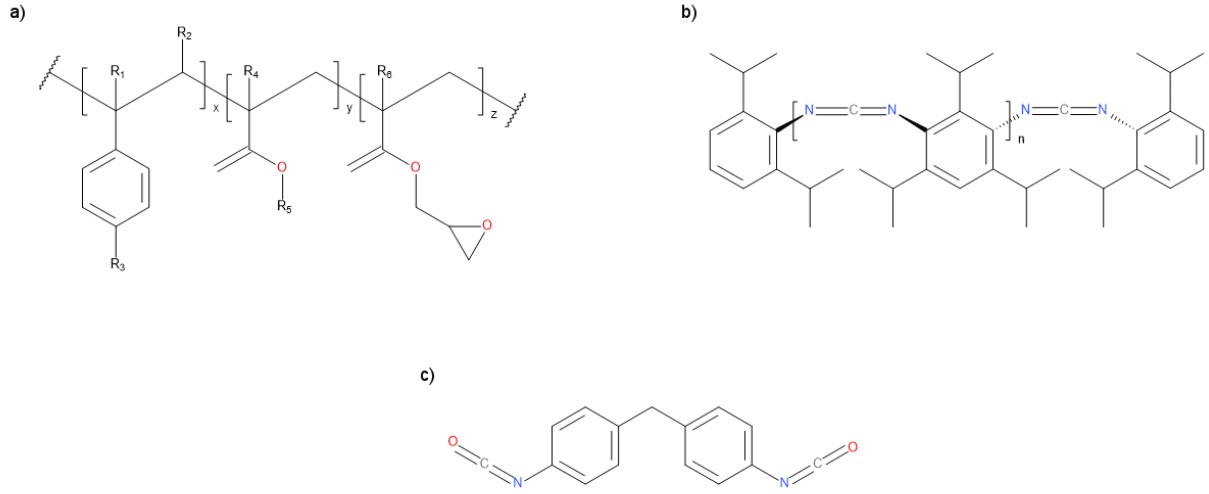

Figure 1. Chemical structure of chain extenders used for PLA modification; poly(styrene-acrylic-co-methacrylate glycidyl) copolymer, **J** (a); bis(2,6-diisopropylphenyl)carbodiimide, **KI** (b); 4,4'-methylenediphenyl diisocyanate **MDI** (c)

2.2. Samples preparation

A polymeric powder with defined granulometric characteristics was obtained through a dedicated grinding and melt mixing process. The PLA cups were comminuted using a GV 270/430 F.lli Virginio slow-speed granulator, getting an average particle size of 6.5 mm. Then, physical mixtures of PLA were prepared with modifiers dosed to the ground polymer in concentrations of 0.3 wt% (J) and 2 wt% (KI and MDI), followed by melt blending in a Zamak EHD 16.2 co-rotating twin-screw extruder (190 °C, 50 rpm). The extrudate obtained ~~in this way~~ was granulated to a length of approximately 5 mm, and then cryogenically ground using a Retsch ZM 200 high-speed mill, using dry ice, at a knife speed of 10,000 rpm and with 800 μm sieve.

The micropellets were rotomolded using a Remo Graf spindle device, using steel molds of 185x60x60 mm, rotating with a speed ratio of 3:1 in two axes, with a batch weight of 120 g. The oven was set at a temperature of 230 °C. The heating stage lasted for 20 minutes and the cooling-was done ~~using~~ under forced air. Before each melt processing, materials were dried at 50 °C for 24 h in a vacuum cabinet dryer.

2.3. Methods

The number-average molar masses (M_n) and the mass-average molar masses (M_w) of PLA samples and polydispersity (D) were determined by size exclusion chromatography (SEC). An Agilent Pump 1100 Series apparatus (preceded by an Agilent G1379A Degasser) equipped with a set of two PLGel 5 μm MIXED–C columns was used for these analysis. Wyatt Obtilab T-Rex differential refractometer (RI) and a Dawn Heleos (Wyatt Technology Corporation) multi-angle laser photometer (MALLS) were used as detectors~~.~~

Viscometric average molecular weights of rotationally molded PLA (M_v) using the Mark Houwink's equation, performing the measurements in an at 25 °C, dissolving the samples at 1 g/d in chloroform (see supplementary materials for more details).

The thermal stability of samples was determined by Thermogravimetric Analysis (TGA) performed in a Netzsch TG209 F1 device using Al_2O_3 crucibles. The samples were heated at 10°C/min from 30 to 900 °C~~.~~ Both weight loss (in %) and first derivative TG curves (dTG) were used for the analysis.

Fourier transform infrared spectra (FTIR) were obtained between 4000 and 400 cm^{-1} wavelength, in a Jasco FT/IR-4600 apparatus, under the attenuated total reflectance (ATR) mode.

The color of the samples was evaluated through L*a*b* coordinates [45], according to the International Commission on Illumination (CIE), using a HunterLab Miniscan MS/S-4000S spectrophotometer.

The yellowness index (YI) was determined following ASTM E 313 standard after recalculation of color parameters to CIEXYZ coordinates.

The UV–Vis spectra analysis (absorbance in the region 190–1100 nm) of the samples was conducted using a UV–Vis Schott UviLine 9400 spectrophotometer.

Differential scanning calorimetry (DSC) analysis was performed on a Netzsch DSC 204 F1 Phoenix instrument with a nitrogen flow of 20 ml/min in aluminum pierced pans. Heating and cooling scans were performed from -30 °C to 200 °C, with a double heating cycle, at a heating and cooling rate of 10 °C/min.

Rheological properties were obtained using an Anton Paar MCR 301 rotational rheometer equipped with a 25 mm parallel-plate, under the oscillation shearing mode at a temperature of 210 °C. The linear viscoelastic region (LVE) was obtained performing in first place the strain sweep experiments. The strain amplitude sweep experiments were performed at the same temperature ~~(210 °C)~~ with a constant angular frequency of 10 Hz in the varying strain window 0.01–100%, with a 1% strain for frequency sweep experiments (~~found~~ in the LVE). The frequency sweep measurements were performed in the 0.05-500 rad/s angular frequency (ω) range. Additionally, the measurements in constant shearing conditions (γ = 1 %, ω = 6.24 rad/s) in an oxidative atmosphere were performed for unprocessed materials in 60 min.

Three-dimensional details of the samples' closed porosity, wall thickness and the spatial position of absolute pores were obtained by computed tomography (CT). An industrial computed tomograph by General Electric v|tome|xs with VGStudio MAX 2.2 software was used, performing the measurements for a voxel size of 100 µm.
The tensile test experiments were conducted in a Zwick Roell Z010 universal testing machine, according to the European standard ISO 527. The samples with dimensions of 10x100 mm were evaluated with a crosshead speed of 1 mm/min during Young modulus determination (up to elongation of 0.2 %), increasing speed to 5 mm/min for the remaining assay. The reported values of tensile properties are the average of at least 7 tests.
The impact strengths of the 10x4x15 mm unnotched samples were obtained by the Dynstat method (DIN 53435), using a Dys-e 8421 apparatus with a 0.98 J hammer, giving results as the average of at least 7 tests.
The hardness evaluation was carried out using a durometer HBD 100-0 Shore D from Sauter GmbH, following the ISO 868 standard. The presented test results represent the averaged values from at least 15 measurements.
The dynamic mechanical properties were studied using DMA under torsion mode for samples with 10x50 mm, using an Anton Paar rotational rheometer equipped with SRF system. The system operated at a frequency of 1 Hz and strain of 0.01 % in the temperature range between 20 °C and 110 °C, with a heating rate of 2 °C/min.
The emissions assessment of the selected aromatic and aliphatic hydrocarbons released to the gaseous phase from the studied materials was performed using the Markes' Micro-Chamber/Thermal Extractor™ – µ-CTE™ 250 (Markes International, Ltd.). Detailed information about the working parameters and overall design of the employed µ-CTE™ 250 system was described elsewhere [49,50]. Emitted analytes from tested materials were collected on a Tenax TA sorption medium placed inside a stainless steel tube (Merck KGaA, Darmstadt, Germany). After sampling process, collected organic compounds were liberated form sorption bed using the two-stage thermal desorption (TD) technique (Markes Series 2 Thermal Desorption Systems; UNITY/TD-100 (Markes International, Inc.). Emitted chemical compounds were analyzed quantitative and qualitatively using gas chromatography (Agilent Technologies 7820A GC; capillary column: J&W DB-1, USA; Data processing system: OpenLAB CDS ChemStation)) technique equipped with flame ionization detector (FID), as described elsewhere [51]. The main representatives of aromatic and aliphatic hydrocarbons emitted were obtained using a certified reference solution, containing 13 representative VOCs in 1 mL of MeOH at a concentration level of 2000 µg/mL each (VOC EPA Mix 2, Supelco, Bellefonte, PA, USA) and n-undecane reference solution for GC (5 mL, Supelco, USA). Identification of VOCs representatives using the TD-GC-FID system was performed comparing the retention times (RTs) of analytes for investigated samples and RTs of chemical compounds which occurs in applied VOCs reference solution. Data received by TD-GC-MS system were compared with data received with the use of TD-GC-FID system. Additionally, for mentioned aliphatic hydrocarbons, their RTs were assessed on TD-GC-FID system using self-prepared mixture containing pure hydrocarbons form n-dodecane to n-tetradecane. The quantification of the VOCs representatives was performed using five-point calibration solutions in range from 2 µg/mL up to 500 µg/mL, as ~~The calibration protocol can be~~ found in detail elsewhere [52]. The

limit of detection (LOD) was calculated using signal-to-noise (S/N) ratio. The average value of LOD parameter was 0.35 ng.
The emitted organic compounds were screened against the mass spectra database (NIST Mass Spectral Library v. 2.0 (2011)), only considering relationships with a probability higher than 80% [53].

3. Results and discussion

3.1. Molecular structure of the PLA

The molecular weight of pure and modified PLA before and after processing, determined by SEC with an RI detector and ~~a~~n MALLS detector, and by viscometric method (VM), are presented in Table 1. Despite keeping the temperature regime at 190 °C and performing a proper drying process, melt extrusion caused a decrease in the molecular weight (M_n, M_w, M_v) of PLA relative to the base material (cup). The incorporation of molecules of the tested CEs into the structure of PLA results in an increase in the molecular weight of PLA. As can be seen from the data contained in the Table 1, the highest increase in PLA molecular weight was observed in the case of using J. The rotational molding process significantly affects the molecular weight of PLA, namely a 20-30% decrease in the molecular weight of the base material was observed due to the two steps processing (i.e. ~~to~~ melt extrusion and subsequent rotomolding). The molecular weight of modified polylactides (various combinations with CEs) despite the initial increase after molding process is also reduced. It is worth noting, however, that when KI is used as a CE~~s~~, the reduction in the molecular weight is the smallest. At the same time, it should be emphasized that the polydispersity (D) in the case of PLA-KI practically does not change, while in the case of PLA-J it increases significantly. This effect may be due to the defragmentation of the significantly branched polymer by adding the styrene-acrylic multi-functional-epoxide oligomer [54] of PLA main chain. The size-exclusion chromatography traces for pure and modified PLA with CEs such as KI and MDI showed symmetrical, monomodal molar mass distributions (Supporting Information, Fig. S1). The bimodal distribution of molar masses in the SEC chromatogram could be observed only in the case of using J as a PLA chain extender (Fig. S1). The trends in the observed changes in the molecular weight of PLA with various CEs before and after processing, determined by different methods, are comparable, despite the different values. Moreover, the observed drops in M_n for unmodified PLA are similar to the elsewhere reported changes for combined extrusion and injection molding for six processing cycles [14]. The lower values of M_n and M_w between RI and MALLS detection results from the technical aspect of measurement and the difference in hydrodynamic volumes between PLA and PS standards with comparable molecular weights [55,56].

Table 1. Molar Masses of PLA samples obtained by SEC with an RI and MALLS detectors, and viscometric method (VM).

Sample		RI			MALLS			VM
		M_n[g/mol]	**M_w[g/mol]**	**D**	**M_n[g/mol]**	**M_w[g/mol]**	**D**	**M_v [g/mol]**
PLA – cup (base material)		86 539	169 374	1,957	81 930	135 700	1,857	149 874
Before	PLA	66 744	135 192	2,026	55 040	91 280	1,658	124 886

	PLA-J	99 305	274 083	2,760	90 640	320 500	3,536	190 894
	PLA-KI	88 100	167 711	1,904	53 060	93 950	1,771	146 983
	PLA-MDI	87 697	169 913	1,938	94 290	157 900	1,674	157 343
After rotomolding	PLA	41 877	80 427	1,921	24 490	41 030	1,675	54 457
	PLA-J	858 898/ 64 928 71 040	977 629/ 128 978 208 345	1,138/ 1,986 2,933	51 490	212 200	4,121	162 421
	PLA-KI	70 860	142 373	2,009	51 410	91 050	1,771	136 604
	PLA-MDI	68 848	126 964	1,844	42 120	72 850	1,730	108 695

3.2. Thermal stability

The TGA was carried out for rotomolded samples; Figure 2 presents the plots for TG and DTG. Additionally, the thermal parameters, i.e., mass loss at 5, 10, and 50 %, residue at 900 °C, and detailed data describing the DTG peaks, were summarized in Table 2. Taking the 5 % mass loss of the sample as the criterion for the onset degradation, it can be concluded that the use of J and KI caused a similar increase in polymers' thermal stability compared to unmodified PLA. At the same time, the incorporation of diisocyanate led to the reciprocal effect. This trend is also observed in the case of higher mass losses; taking into account the values measured in the range corresponding to the processing temperature, the sample modified with KI differs in the curve course from other material series. It may be attributed to the partial degradation of the modifier itself (maximum processing temperature 200 °C recommended by the manufacturer). A similar effect of decreased thermal stability of PLA modified with Bioadimide® 100 was reported by Laske et al. [57]. It should be emphasized, however, that the values of degradation temperatures are much higher than the commonly used processing temperatures of PLA [58]. It is assumed that extending the chains' length causes a reduction in the number of the active site of chain ends, which translates into a decreased intensity of depolymerization from back-biting resulting in slower PLA degradation [59].

An interesting phenomenon was observed in the analysis of the peak of DTG shift (Fig. 2). For the PLA-KI and PLA-MDI samples, a different course of curves was noted, with the appearance of an additional peak at a lower temperature, in the range of an overlapping inflection of the curve observed for PLA and PLA-J samples at 347 °C. At the same time, rheological results suggest the creation of a thermally stable three-dimensional network in the case of MDI use. According to Yang et al. [60], who described significant thermal stability improvement of the PLA cross-linked with triallyl isocyanurate when dicumyl peroxide is present as initiator, it can be stated that the used modifier does not cross-link rotomolded PLA parts. The thermally stable structures, which also improves ~~improving~~ the viscosity of the formulations ~~compositions~~ after ~~processing~~rotomolding, are instead the result of dispersed rigid domains of aromatic isocyanates or the creation of local thermally stable cross-linked PLA-MDI networks. A comparable shift in the maximum DTG curve was noted for PLA grades subjected to thermooxidative and thermomechanical degradation [20]. The observed double peak and the other inflection in the curve may result from increased polydispersity after the rotomolding process and degradation of only part of the polymer material. The degradation phenomena are

observed as decreased molecular masses, not from the phenomena induced by thermal degradation, but from thermooxidative and hydrolysis reactions during melt processing [20,61].

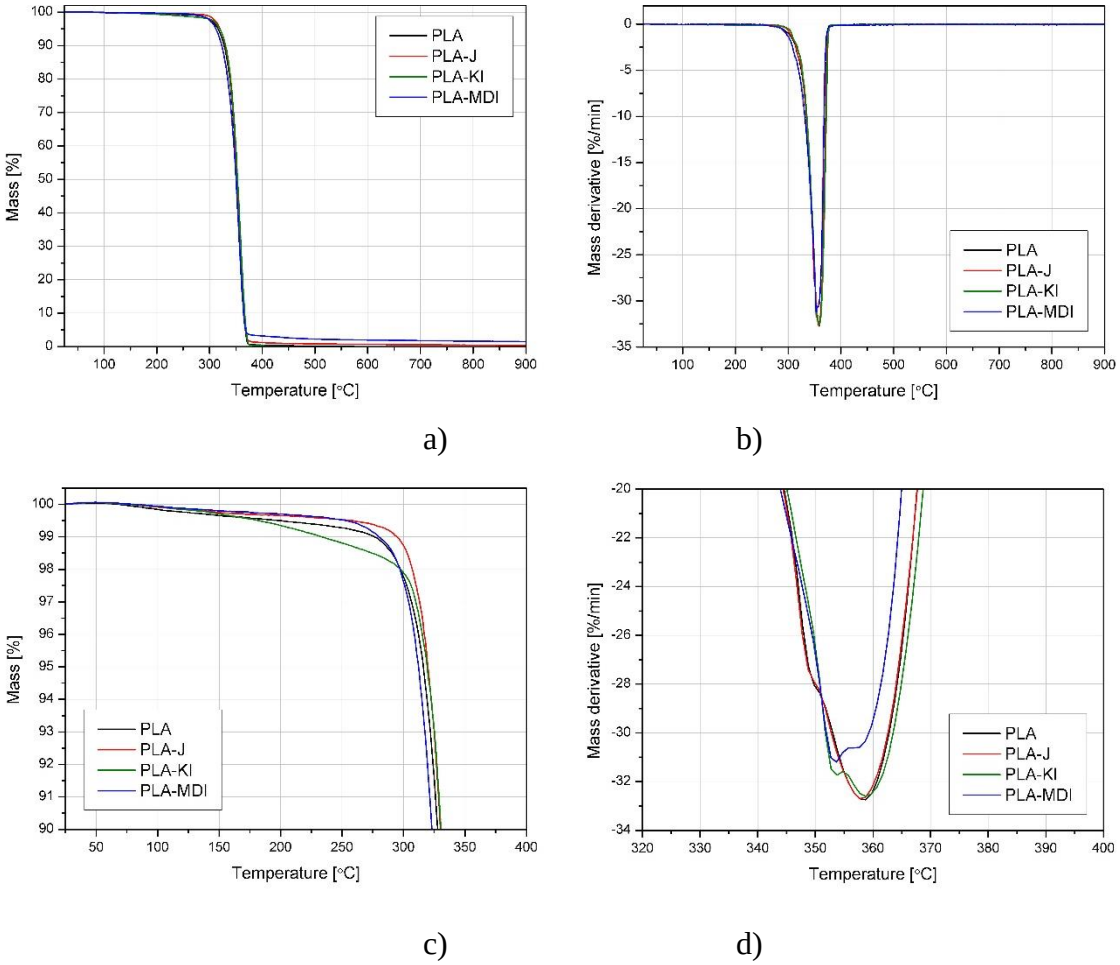

Fig. 2. TG and DTG curves of samples taken from rotomolded parts made of pure and modified PLA: a) TG, b) DTG, c) TG for a maximum of 10 % weight loss, d) DTG for the temperature range at which maximum degradation rate occurs

Table 2. Thermal parameters obtained by TGA.

Material	$T_{5\%}$	$T_{10\%}$	$T_{50\%}$	Residue at 900°C	DTG peak
	[°C]			[%]	[%/min, °C]
PLA	316.1	327.8	352.1	0.41	-32.75, 358.4
PLA-J	319.9	330.0	352.6	0.36	-32.72, 358.0
PLA-KI	319.3	330.5	353.2	0.54	-32.60; 358.7
PLA-MDI	312.0	323.1	350.3	1.47	-32.25; 353.3

3.3. FTIR spectroscopic analysis of compounds and modified PLA

Figure 3 shows the compiled FTIR spectra of the raw PLA sample taken from the unprocessed product (cup before recycling) and the chain extenders used for its stabilization. The FTIR spectrum of unprocessed PLA consists of the typical for this polymer absorption bands from its chemical structure, i.e., asymmetrical and symmetrical (2997 cm^{-1} and 2946 cm^{-1}, respectively)~~()~~ stretching of –CH–, carbonyl stretching (1748 cm^{-1}), methyl -CH_3 bending

(1456 cm^{-1}), both symmetric and asymmetric bending on -C-H- deformation (1382 and 1360 cm^{-1}), -C=O bending (1263 cm^{-1}), -C-O- stretching (1181, 1127 and 1079 cm^{-1}), hydroxyl bending (1047 cm^{-1}), -CH_3 rocking (956 cm^{-1}), and, finally, -C-C- stretching (867 cm^{-1}) [62–66]. The spectra of the Joncryl® (J) show the presence of most prominent peaks at a wavelength of about 1250 cm^{-1}, 910, and 850 cm^{-1}, 760, and 710 cm^{-1} that are associated with stretching vibrations of the epoxy group (CH_2-O-CH). The peaks at the wavelength of 1455-1601 cm^{-1} are related to the C-C stretching in the phenyl group. The peak at a length of about 1720 cm^{-1} confirms the presence of the C=O group. The absorption band at a wavelength of about 3026 cm^{-1} is related to the stretching vibration of the Ar-H moiety of the phenyl group, while peaks in the wavelength range of 3000-2800 cm^{-1} indicate the presence of CH_2 and CH_3 groups [67]. BioAdimide® 100 (KI), often used as a stabilizer against thermoplastic polyesters hydrolysis, is characterized by a more complex FTIR spectrum than Joncryl. The band at about 3000-2800 cm^{-1} wavelength is related to the occurrence of CH_2 and CH_3. The peak at a wavelength of about 2100 cm^{-1} shows the presence of -N=C=N- groups, while the absorption bands observed at a wavelength of approximately 1600-1500 cm^{-1} are attributed to the presence of -NH_2 (1620 cm^{-1}) and NH (1520 cm^{-1}). The peaks confirm the C-N moieties at 1460-1350 cm^{-1} and 1250 cm^{-1}. The peak at the wavelength of 600 cm^{-1} may be associated with the C-N-C and C-C-N groups [31,33]. MDI is a diisocyanate containing two phenylene rings with one methylene group between them [68]. The spectrum presented in Fig. 3 shows the most intense doublet absorption band at 2273 cm^{-1}, reflecting the asymmetric stretch of the isocyanate group (N=C=O). Moreover, several absorption bands characteristic of MDI were also noted, including the NO_2 aliphatic group at 1729 cm^{-1}, carbonyl group CO at 1608 cm^{-1}, asymmetric nitro compounds at 1524 cm^{-1}, CO alkoxy stretching at 1102 cm^{-1}, aromatic sp^2 CH bending at 814 cm^{-1}, and sp CH bending at 624 cm^{-1} [69].

FTIR spectra of unmodified and chain-extended PLA before and after the rotomolding process are presented in Figure 4. All spectra of PLA samples before and after processing are similar. For the CE-modified series, no new distinct peaks have been denoted, while some changes in the intensities of the characteristic PLA absorption band were noted, i.e., C=O and -C-O- stretching. The effect of most intensively increasing absorbance in the carbonyl C=O range for all material series after processing can be referred to dominant thermooxidative degradation during long-term melt processing [20]. The reaction that occurs because of the application of Joncryl® is based on the ring-opening of the epoxy groups towards PLA carboxyl or secondary hydroxyl groups and the creation of new covalent bonds [70]. Due to the complete reaction of epoxy -C-O-C- groups and the small additive content used in the case of PLA-J, additional absorption bands were not visible. For the Bioadimide, the reactions of carboimide -N=C=N- groups with carboxyl and hydrogen bonds at the polymer backbone or providing to transesterification of the PLA chains results in the creation of similar amide groups N-C, which one might expect to appear in the absorbance range between 1250-1000 cm^{-1}. The additional peak in the PLA-KI spectrum has probably too low intensity and overlaps with more distinct bands from the PLA. Finally, for the PLA-MDI, there were no peaks already for micropellets in the range around 2273 cm^{-1}, attributed to the presence of unreacted N=C=O groups. So, it can be concluded that MDI reacted with free hydroxyl and carboxyl end groups of PLA forming amide bonds [35] during the mixing at molten state for the production of micropellets. The presence of urethane bonds cannot be confirmed in this case due to overlapping with PLA

characteristic bands [71]; however, increasing the intensity of the mentioned early bonds may be a confirmation. The FTIR analysis led to an ambiguous description of the reactivity of the proposed systems and the structural changes of PLA caused by the CE due to the overlapping of absorption bands and the low ratio of modifiers used. Oscillatory rheology (section 3.6) is used as a more powerful analytic tool to describe the interactions and degradation processes arising.

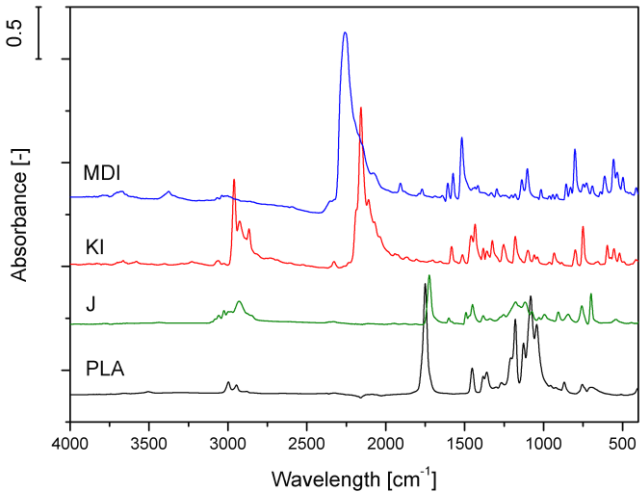

Fig. 3. FTIR spectra of chain extenders and unprocessed PLA.

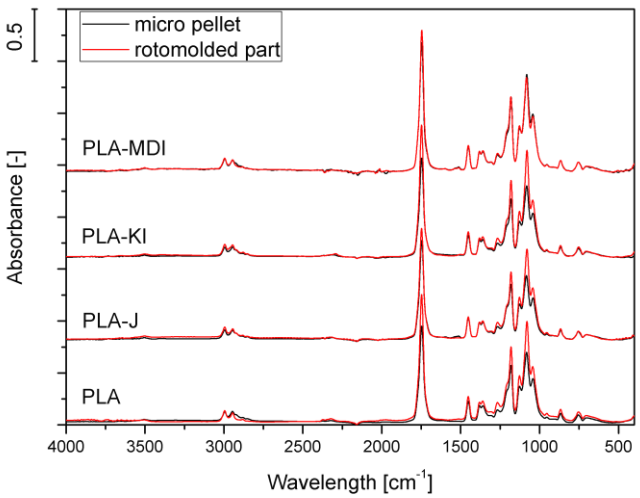

Fig. 4. FTIR spectra of pure and modified with CE PLA before and after the rotational molding process.

3.4. Color analysis

Although the color change induced by degradation processes cannot be treated either as a quantitative parameter, which indicates the main degradation mechanism or in a linear manner to describe the changes in the polymer structure, its evaluation can qualitatively supplement the analysis of the potential structural changes [72]. Table 3 shows the results of color measurements with the parameters calculated based on processing the data contained in the

CIELab space following the formulas (3,4) and measurements made using UV-Vis spectrophotometry. Additionally, Figure 5 shows the UV-Vis spectra for rotomolded samples. The reference sample was a PLA cup before the recycling procedure. The total color change has been determined in reference to the rotomolded PLA series. It can be observed that the most distinct differences in relation to the material not subjected to rotomolding were noted in the case of changes in the luminescence L and chromatic parameter and b*, which is associated with the sample darkening and yellowing. Increasing the value of the chromatic parameter b* is related to polymer degradation phenomena in many cases [73]. This information is completed using the quantitative analysis presented by the YI calculated according to the formula (4). The YI had a significant difference for all processed materials compared to unprocessed PLA, which had a negligible value of 0.81. For the batch containing MDI, an almost as substantial increase in YI as for the unmodified PLA was observed. The total color change, in all cases, exceeds the value of 5, so these materials are characterized by a very intense color change. Additional pigments will therefore be necessary when molding products even from effectively stiffened varieties of recycled PLA. Both the technological process and the use of chain extenders resulted in decreased PLA transparency. In the case of unmodified PLA and PLA modified with diisocyanate, the restriction of transparency resulted not only from the yellowing of the polymer due to degradation phenomena but also from the air inclusions within their structure.

Table 3. Results of color evaluation; CIE *L*a*b** chromatic parameters, total color change, and yellowness index.

Material	***L****	***a****	***b****	**Δ*E***	**Yellowness index (YI)**	**Transparency (A_{600}/mm)**
PLA – cup (base material)	89.43	0.81	0.11	-	0.81	539.86
PLA	52.52	7.82	22.43	-	68.19	23.93
PLA - J	69.04	4.78	17.05	17.64	45.36	7.94
PLA – KI	52.48	3.46	12.79	10.60	40.32	9.67
PLA - MDI	41.84	8.44	18.42	11.42	69.44	0.28

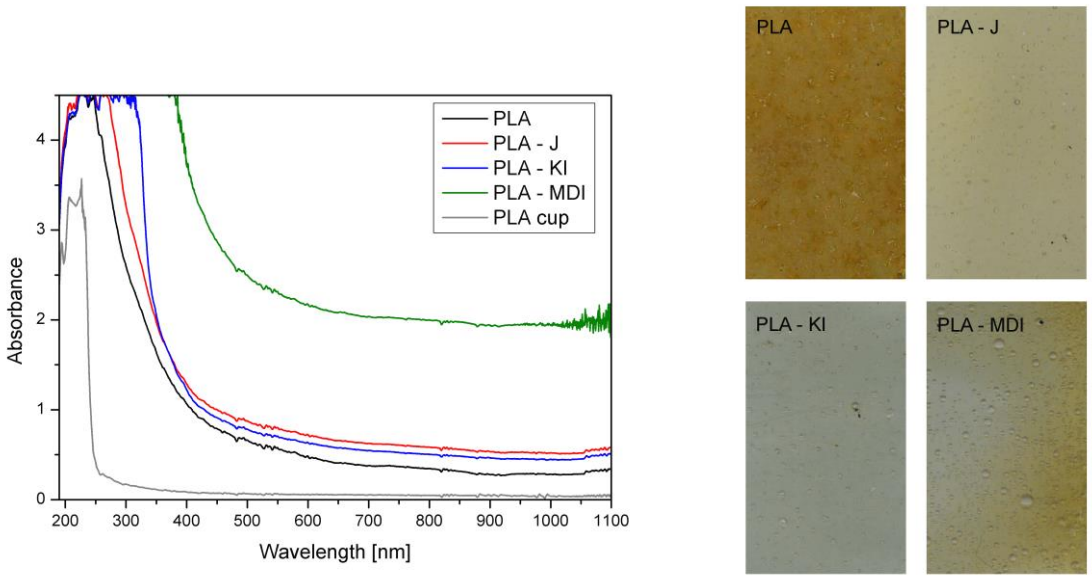

a) b)

Fig. 5. UV-Vis spectra of rotationally molded samples made of unmodified and stabilized PLA (a), the appearance of the external surface of rotomolded parts (b).

3.5. Thermal properties

The results of the thermal analysis carried out by the DSC method of polylactide before and after the rotational molding process are summarized in Table 4, which shows the results for the glass transition (T_{gDSC}), cold-crystallization (T_{cc}), and melting (T_m) temperatures, enthalpies of cold crystallization and melting (ΔH_{cc}, ΔH_m) taken from second heating, and crystallinity (X_c) calculated according to equation (2). Additionally, the DSC thermograms for samples taken from rotomolded parts, showing changes in heat flow during both heating and cooling processes, are presented in Figure 6.

The observed lack of influence of processing in the harsh temperature-oxidizing environment and degradation phenomena on thermal properties evaluated by DSC indicates a content of the D-PLA enantiomer in PLA-cup waste [16]. Polylactides from this grade, as ~~was~~ described ~~before~~ earlier [15,20], became utterly amorphous, and the T_{gDSC} observed in the thermograms did not change. In the considered case, the glass transition temperature T_{gDSC} reveals no significant changes caused by the influence of the technological process. As shown by Cuadri and Martin-Alfonso [20], thermal and themooxidative degradation did not lead to a noticeable reduction in T_{gDSC}, as would be expected, taking into account the mechanism of chain scission. In the case of the rotomolded unmodified PLA sample, the presence of two peaks on the second heating curve was noted. This effect may be related to the significant degradation and change in its structure. While the used polymer is characterized by an almost amorphous structure in the solidified state, the course of the melting curves recorded for PLA showed a double peak, which can be attributed to the melting and/or recrystallization of metastable crystals, the reorganization and melting of α'-form into stable α-form crystals, or the melting of crystals with different lamellar thickness [74]. At the same time, this phenomenon is observed for various semi-crystalline polymers and may be related, as in the considered case, to a significant change in the molecular weight of the polymer [75,76]. One of the explanations for the appearance of

multiple melting peaks is the irreversible melting process of metastable crystalline forms originating from metastable crystal forms, thin lamellae, and crystal defects [74]. The T_m of chain-extended PLA with KI and J series did not change after processing, unlike PLA-MDI. The increase in melting temperature for the MDI in the second heating curve would confirm the creation of a highly branched partially permanently cross-linked structure [22]. The degradation process led to the development of smaller molecules that exhibit a more accessible arrangement during solidification [77]. The extension of PLA chains with high D-PLA content resulted in increased branching and lowered PLA crystallinity [22]. As also demonstrated in the rheological evaluation, the incorporation of J and MDI increased the ~~of~~ polymer long branches and~~,~~ resulted~~s~~ in a decrease in the tendency to crystallization; this was~~,~~ observed as a reduction of both cold crystallization and melting enthalpies of modified versus unmodified PLA in DSC heating thermograms.

It should be emphasized that only in the case of polylactide without any modification the increase in the degree of crystallinity was noticeable for the rotomolded samples. The modified samples showed almost null crystallinity, and materials should be treated as amorphous. Discussed data from DSC experiments were taken from second heating to exclude the influence of process conditions and compare the material's structure. However, taking into account the curves of the cooling stage, where no exothermic peaks were found for any of the samples, it can be stated that the obtained increased degree of crystallinity of the unmodified PLA, expected to be strongly degraded, is due to the easier reorganization of short macromolecular chains rather than from the phenomena of creating ordered~~ly~~ structures from the melt during non-isothermal crystallization.

Table 4. Calorimetric parameter characterizing thermal behavior of the samples measured during the 2nd heating.

Material		***Tg***	***Tcc***	***Tm***	**Δ*Hcc***	**Δ*Hm***	***Xc***
		[°C]			**[J/g]**		**[%]**
Before processing	PLA	60.7	114.9	149.6	31.93	32.39	0.5
	PLA-J	61.3	116.4	149.6	25.85	28.24	2.6
	PLA-KI	58.7	114.8	148.1	28.33	30.16	2.0
	PLA-MDI	61.0	118.8	150.4	28.21	30.59	2.6
After processing	PLA	59.1	114.3	148.1 154.3	35.68	43.81	8.7
	PLA-J	60.3	116.3	149.6	32.63	32.71	0.1
	PLA-KI	59.3	115.5	148.7	27.70	28.83	1.2
	PLA-MDI	61.3	118.1	153.5	34.92	35.53	0.7

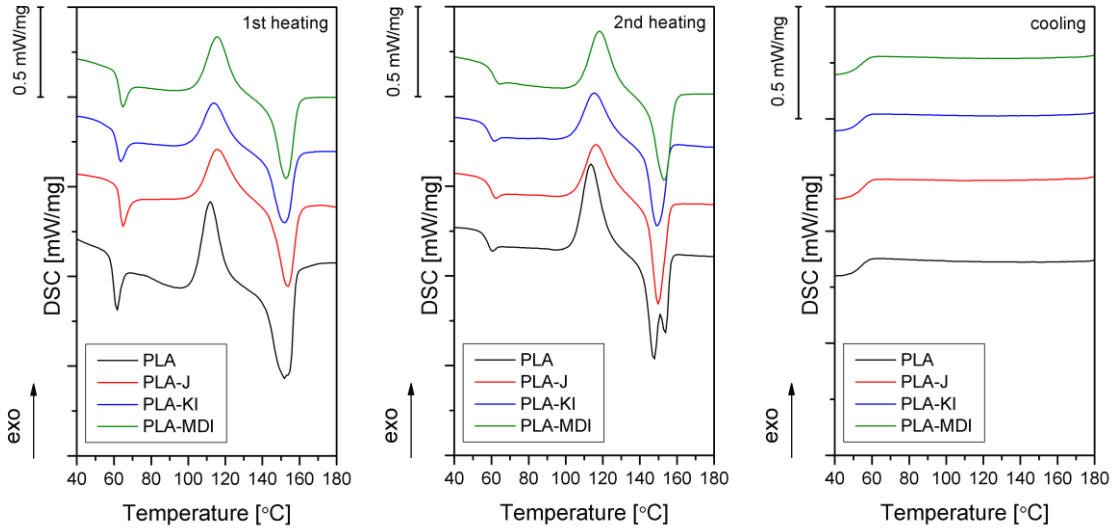

a) b) c)

Fig. 6. DSC curves of pure and modified PLA after rotational molding process, for a) first heating cycle, b) second heating cycle and c) cooling stage

3.6. Rheological and processing properties

Oscillatory rheology is a powerful measuring tool that describes the rheological properties of polymers and indirectly evaluates the effectiveness of modifiers, allowing for determining the extension of the structural changes due to degradation or grafting. Figure 7 presents the thermomechanical curves showing the changes in the storage (G') and loss (G'') moduli for micropellets (Fig. 7a) and samples taken from rotomolded parts (Fig. 7b). The complex viscosity curves before and after the rotational molding process are presented in Fig. 7c. The additional G' and G'' curves presented as a function of time, recorded during measurements carried out under steady shear conditions and constant temperature and in an oxidizing atmosphere, are plotted in Figure 7d. A change in the effectiveness of the impact of individual modifiers can be noticed, based on the analysis of the course in G' modules analyzed for materials before and after their processing (Fig. 7a,b). The plateau on the G' curve observed for PLA-J and PLA-MDI in the angular frequency range below 1 rad/s can be interpreted as the formation of stable 3D structures hindering the mobility of macromolecules. At the same time, in the case of PLA-J samples, this behavior disappears after rotomolding. Therefore, it can be concluded that in the case of J-modified PLA, the molecular weight is improved, reflected by the limited mobility of macromolecules in the range of low angular frequencies. However, this additive is not limiting the thermooxidative degradation, as the rheological effects observed for micropellets are not observed for the rotomolded parts.

In contrast, PLA-MDI leads to the formation of temperature-stable cross-linked structures, confirmed in MFI analysis, as discussed later. The storage modulus and complex viscosity curves of PLA-MDI exhibit the typical course for cross-linked PLA, according to studies by Wu and co-workers [78]. An interesting rheological behavior occurs for KI-stabilized PLA: the curves for the materials before and after the forming process did not change. Considering the minor differences in the measured molecular weight of PLA-KI before and after processing and

the similar rheological behavior, it can be concluded that the KI showed the highest modification efficiency. KI did not significantly modify the PLA structure during melt mixing and only reacted during degradation changes caused by thermooxidative or hydrolytic degradation occurring during rotational molding. No increase in viscosity in the polymer powder due to the modification was observed, so any change regarding the removal of air residues and voids formation is expected during the densification [79]. Therefore, KI was the only compound not adversely affecting the processing parameters of PLA while stabilizing its structure, confirmed by the lack of significant changes in the rheological properties and molecular weight before and after long-term processing.

The main difference between the samples with branched and cross-linked structures (PLA-J and PLA-MDI) and linear materials (PLA, PLA-KI), observed on the curves representing changes in *G*' and *G*" recorded during the experiment carried out with constant shearing (Fig 7d), can be seen in the changes of the *G*' curve slope. The materials described as linear showed a significant discrepancy between the dominant share of viscous and elastic properties. While the J- and MDI-modified PLA series reveal the characteristics of visco-elastic liquids, with the values *G*' and *G*" close to each other, the linear materials show a predominant viscous behavior, with *G*" values significantly higher than *G*'. Interestingly, the branched materials show a different behavior between them, as seen from the different course of the *G*" curves for PLA-J and PLA-MDI, which suggests a difference in the stabilizing behavior between those series. The simultaneous reduction of the *G*" value as a function of time with an almost unchanged *G*' course suggests a gradual defragmentation of the polymer chains while limiting their mobility due to stiff and cross-linked structures. The results show that MDI-modified PLA increased its molecular weight but did not prevent the degradative effects of processing. For PLA-J, the decrease in both curves is similar and less pronounced, which might be related to a better stabilizing effect of this additive.

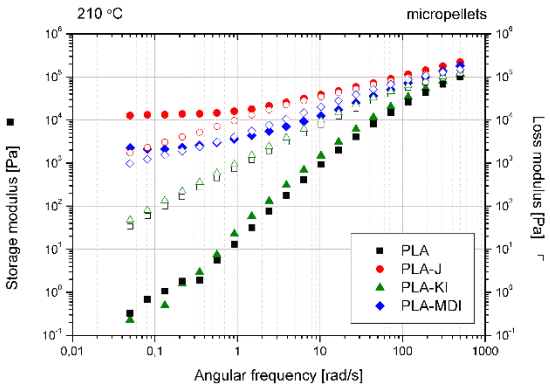

a)

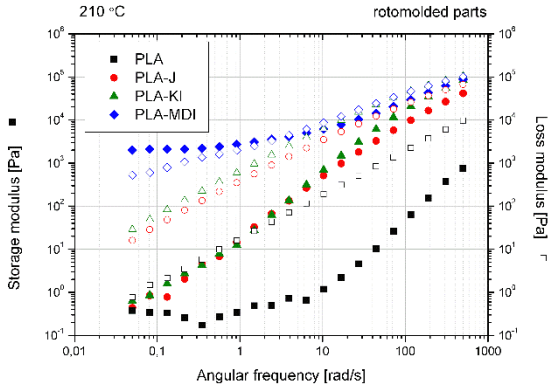

b)

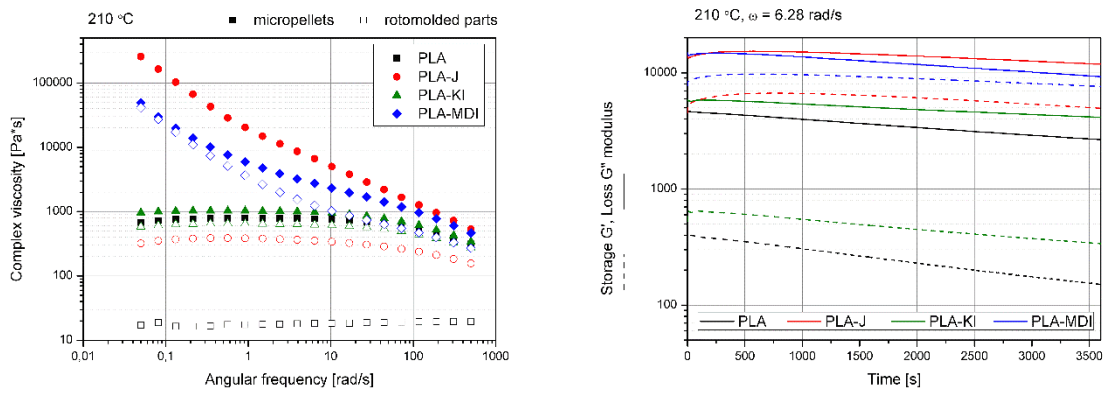

c) d)

Fig. 7. Storage (G') and loss (G") moduli and complex viscosity curves taken from frequency sweep experiments (a-c); G' and G" vs. time measurements obtained during constant-shear oscillatory experiments in the oxidative atmosphere for pure and modified PLA micropellets (d).

In order to verify the description of changes in the macromolecular structure of PLA subjected to stabilization and the durability of the effects of increasing the molecular mass and the presence of long chain branches (LCB) or the presence of permanently cross-linked intermittent structures, rheological data were presented in the form of van Gurp-Palmen plots (vGP). According to previous studies, this method of interpretation of oscillatory rheological data is sensitive to polymer molecular weight and polydispersity changes [80]. Therefore, it correlates with the mechanism of increasing PLA main chains' length and the LCB formation of PLA modified with different CEs [31,81]. It is assumed with increasing molecular weight, the decrease of minimal values of phase angle (δ_{min}) are noted [82]. At the same time, the complex modulus (G^*) observed in the δ_{min} range decreases with increasing molecular weight [80]. The vGP plots of pure and modified PLA before and after the rotational molding process are presented in Figure 8. Due to the range of angular frequencies used and measurement constraints, the δ values were not covered in the minimum of the potential full range vGP curve, converging the inflection point in the high G^* range. For unmodified PLA and PLA stabilized with KI, the vGP curves show the characteristic for which the curve reaches the δ of 90° for low G^* values, which confirms the dominant viscous behavior [81,83]. The unmodified PLA after processing showed no termination regime, which reflects a significant degradation and the dominant effect of main chain scission and is in line with the results of the SEC and viscometry average molecular weight measurements.

The highly branched structure of PLA-J, with a significantly increased molecular weight, shows entanglement of the long chains that provide rheological effects similar to those usually observed for composites with high filler content, mainly reaching the rheological percolation threshold [84]. However, this effect disappears after the technological process. The degradation effects shortened the macromolecules, restoring the rheological characteristics to that of the linear polymer, such as unmodified PLA before processing. The inflection of the vGP curve for PLA-J in the δ range between 60-80°, observed for the rotomolded samples, suggests that some branching of the PLA macromolecular chains is preserved [81]. Only the PLA-KI reveals vGP

plots almost invariability before and after processing. Therefore, it can be confirmed that the second reaction mechanism proposed by Yang et al. [33] occurs, i.e., the carbodiimide groups react with the backbone of the PLA chain. However, the functional groups were not entirely consumed during the extrusion process, allowing further reaction during the rotational molding. In effect, the chain scission caused by the degradative processes was limited by the transesterification of the PLA chains, leading to its linearization without creating side branches [31]. Finally, MDI-modified PLA showed a similar curve for samples before and after processing. Taking into account that the molecular weight of the polymer decreased and the shape of the vGP plot has retained the shape indicating no dominant share of viscous properties and the presence of physically or chemically related structures in polymer bulk, it can be concluded that the rigid domains of the cross-linked PLA-MDI are a steric hindrance in the polymer. However, they do not protect its structure against degradation effects. Thus, MDI cannot be regarded as an effective chain extender for the valorization process of PLA waste in the rotational molding process.

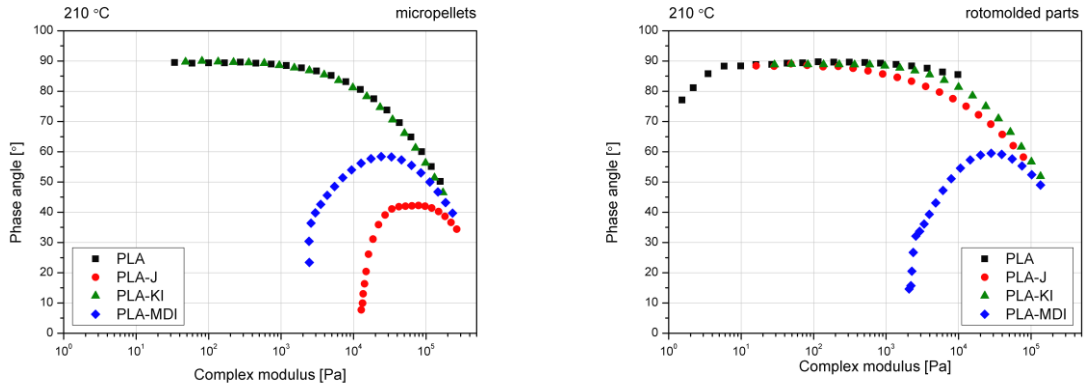

a) b)

Fig. 8. Van Gurp-Palmen plots made based on rheological measurements of a) micropellets and b) rotomolded parts made from PLA and stabilized PLA.

Table 5 summarizes the results of the processing properties measurements through the melt flow index (MFI) analysis. Micropellets processed in the extrusion process and samples from the rotomolded parts were measured at the processing temperature (190 °C) and the temperature described in the ISO 1133 standard and presented in the PLA manufacturers' datasheet (210 °C). The negative influence of the processing on the MFI results of PLA is visible. The unmodified PLA showed an almost 20-fold increase in MFI due to the rotomolding process. The changes in MFI induced by processing-related degradation effects are much higher than those obtained due to multiple processing cycles of extrusion and injection molding reported in the literature [15,85]. This suggests an absolute necessity to use chain extenders in rotational molding, bearing in mind that the recommended MFI value for rotational molding materials is between 2-8 g/10 min [86]. The three chain extenders used in this work significantly reduced this effect. The MFI values of the powders before the rotomolding process were in the range of acceptable values for this technology, while the samples after shaping did not show MFI values significantly higher than the reference PLA, despite the decrease in viscosity already analyzed. This effect confirms that the selected CE compounds and dosages were correct and did not

cause limitations in the process possibilities. The obtained data are consistent with the results presented in the literature [59,87] and oscillatory rheological measurements.

Table 5. MFI results made for material samples before and after processing.

Material	Before rotomolding		After rotomolding
	$MFI_{190°C}$ [g/10 min]	$MFI_{210°C}$ [g/10 min]	$MFI_{190°C}$ [g/10 min]
PLA	10.10 ± 0.60	25.16 ± 1.27	192.47 ± 9.13
PLA - J	1.94 ± 0.17	3.86 ± 0.33	11.47 ± 0.51
PLA - KI	5.88 ± 0.30	15.39 ± 1.34	10.47 ± 0.84
PLA - MDI	2.01 ± 0.40	5.87 ± 0.77	6.68 ± 0.86

3.7. 3D computed tomography

The primary influence on the formation of the porous structure in rotomolded parts has the initial stage of air release [88]. Therefore, the evaluation of changes in molecular weight and the resulting rheological behavior of polymer melts are crucial to understanding the origin of the structural defects in rotomolding. By analyzing the changes in the structure of rotomolded parts evaluated by 3D CT (Fig. 9), it can be concluded that the PLA series modified with polycarbodiimide was characterized by the most favorable structure, with homogeneous wall thickness and a limited number of pores. In the case of unstabilized PLA, pores in thin-walled parts resulted from both degradation processes and an excessive drop in viscosity, generating a laminar flow during the processing. The structural defects observed for the PLA-J and PLA-MDI series result from a significant viscosity increase as an effect of the higher molecular weight of PLA and due to the restrictions in the removal of air entrapped between polymer powder after preliminary sintering into the interior of the part, as well as further diffusion of the air into polymer [88].

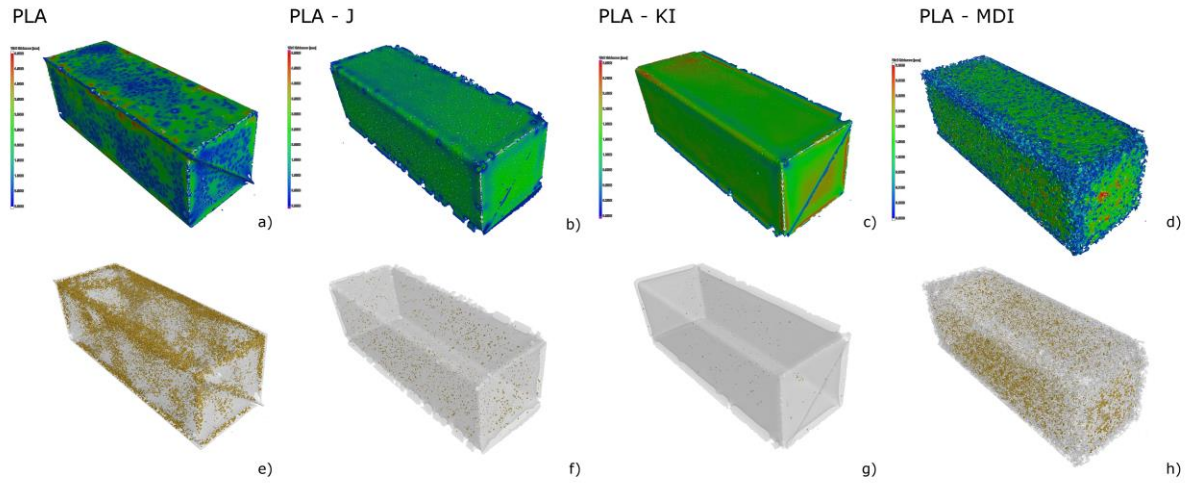

Fig. 9. 3D computed tomography of rotationally molded parts made of pure and modified PLA; wall thickness (a-d), pores distribution (e-h).

3.8. Mechanical behavior

The mechanical properties of rotationally molded products were determined by tensile and experiment, Charpy impact test, and hardness measurements. The results are collectively summarized in Table 6. Rotomolded parts made from unmodified waste PLA were characterized by low mechanical parameters. This is due to the significant degradation leading to changes in the material's structure, as well as the appearance of a large number of pores and uneven distribution of the material in the product, as a result of the drastically reduced viscosity and the release of volatile decomposition products. Adding Joncryl® and polycarbodiimide chain extenders reclaim the mechanical properties of PLA at a level that allows the treatment of the rotomolded products manufactured with their use as construction materials. Both stabilizations make tensile strength three times higher in comparison to unmodified PLA. At the same time, the elasticity modulus for those series was increased. From the point of view of the most crucial disadvantage of PLA, which is low impact strength [89,90], using KI and J allowed for improving this mechanical parameter. Most studies concern the modification of the PLA with various thermoplastic elastomers (TPE) and chain extenders [91]. However, in the case of compositions modified only by KI, an increase in elongation at break and tensile strength of PLA was shown by the addition of polycarbodiimide; the toughness and impact strength were not discussed. At the same time, the ductility can be related to the toughness determined based on the formula (5). Considering the harsh process conditions, degradation changes in the unmodified PLA, and low crystallinity of the polymeric matrix, PLA-KI was characterized by an outstanding impact strength and toughness, mainly because no elastomeric segments were introduced. For samples collected in the rotationally molded PLA-KI part, an over tenfold increase in toughness and eightfold impact strength was demonstrated. Considerable improvements in mechanical properties, including tensile and impact strengths, were observed for the modified KI material series, explained by the high reactivity of KI, which allows both chain-extension mechanisms to occur by joining the OH or COOH groups of PLA terminal, and the moisture residues, which significantly decrease hydrolytic degradation during processing [33]. The addition of PLA cross-linking diisocyanate caused the lowered elasticity modulus, tensile strength, and impact properties of PLA-MDI, resulting from many structural defects in the form of air inclusions (Fig. 9) [92,93].

The Shore D hardness measured for rotationally molded parts did not show a comparable trend. Joncryl-modified PLA was characterized by an increase in hardness of 3 °ShD, while PLA-KI and PLA-MDI samples had lower hardness than unmodified PLA. It should be emphasized that, taking into account the high values of the standard deviation, the changes are insignificant, and the hardness of all materials has not deteriorated significantly, especially if considering the values presented in the literature for amorphous PLA grades (~78 °ShD) [94]. To sum up, the degradation effects occurring in the conditions of the rotomolding, regardless of their dominant share (hydrolytic or thermooxidative), lead to unfavorable changes in mechanical properties, translating into a reduction in tensile and impact strengths. The increased values of these two parameters will be the most important from the perspective of the good stabilizing effect of the applied modifiers.

Table 6. Mechanical properties of PLA rotationally molded products.

Property		PLA	PLA - J	PLA - KI	PLA – MDI
Tensile strength	MPa	15.50 ± 2.80	43.20 ± 2.50	47.70 ± 2.90	21.20 ± 6.40
Elasticity modulus	GPa	2.34 ± 0.25	2.48 ± 0.17	2.65 ± 0.15	1.52 ± 0.31
Elongation at break	%	0.66 ± 0.07	2.10 ± 0.08	2.20 ± 0.09	1.81 ± 0.27
Toughness	J/mm^3	5.36 ± 1.61	55.55 ± 3.39	61.49 ± 8.01	26.34 ± 11.40
Dynstat impact strength	kJ/m^2	1.06 ± 0.56	3.41 ± 1.18	8.12 ± 2.28	1.34 ± 0.61
Hardness	°ShD	77.80 ± 4.90	81.40 ± 2.60	72.80 ± 5.60	74.00 ± 4.90

3.9. Thermomechanical behavior

The results of thermomechanical tests obtained by DMA were summarized in the form of curves illustrating changes in storage modulus (G') and damping factor (tan δ) as a function of the temperature (T) in Figure 10. The course of the G' curves is similar for all series and is characterized by three regions. Plateau ranges from low temperatures to the onset of α-relaxation, coinciding with the glass transition of the PLA. Then, a sharp decrease in the material's stiffness, caused by the increase in the mobility of macromolecules, and the ~~growth~~ increase in G' observed in the range from 90 to 100 °C, resulting from the cold crystallization phenomenon. The lack of changes in the course of $G'(T)$ curves in the range of the glass transition temperature results from the limited ability of the used PLA ~~type~~ grade to create crystalline structures. Despite degradation phenomena and changes in molecular weight, no significant increase in crystallinity occurs for the rotomolded samples, which would cause the adverse effects of softening the amorphous phase of the polymer in the glass transition temperature range. Usually, the tensile test results and the DMA method are assumed to correlate [95]. For all samples, the changes in G' stiffness are performed in the glassy state, with changes in the elasticity modulus assessed using a tensile experiment.

In contrast with the DSC results, the glass transition temperatures (T_{gDMA}) determined as the peak of the tan δ curve from DMA for all materials turned out to be higher than for the unmodified PLA. The noticeable increase in the maximum on tan δ curves in the range of PLA α-relaxation was interpreted as changes in glass transition temperature. This effect is caused by an increase in molecular weight, which reduces free chain ends and free volumes and ~~which~~ makes chain mobility easier, or by the introduction of high amount of aromatic structures, which could also restrict chain mobility (in the case of PLA-MDI) [35]. Moreover, the maxima of α-relaxation curves were characterized by higher values of tan δ for PLA-KI and PLA-J, which may be connected with the reported increased ductility of the materials resulting from the modification of PLA structure. The different tendency in the case of PLA-MDI (reduction of tan δ at peak) may be attributed to the presence of dispersed cross-linked stiff domains, determined from thermal, mechanical and rheological analysis, although may contradict the reduced value of G' in the temperature range below T_{gDMA}. However, the high content of air inclusions, as found in μCT assays, in the structure of the sample taken from the rotomolded part could also explain the lower storage modulus found for this material with respect to the J- and KI-modified ones.

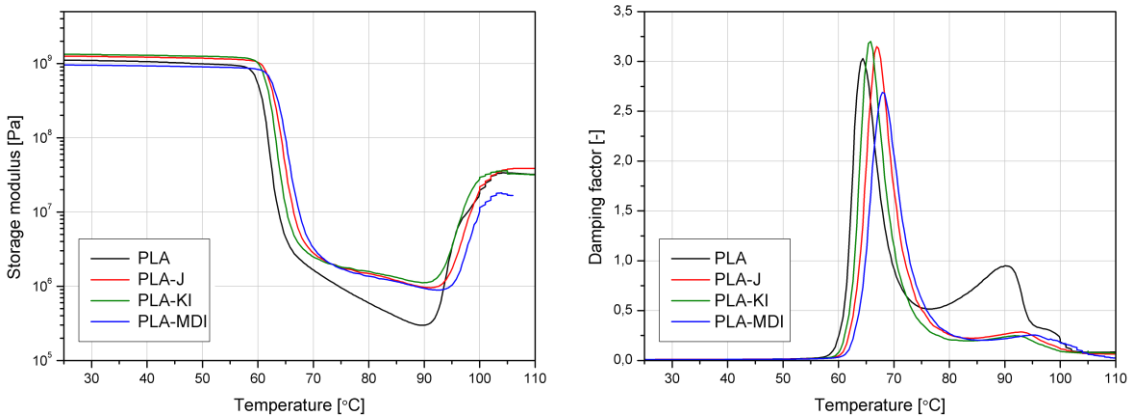

a) b)

Fig. 10. DMA results for rotationally molded pure and modified PLA: a) storage modulus (*G'*) and b) damping factor (tan *δ*) vs. temperature.

3.10. Representatives of volatile organic compounds emissions estimation

A vital issue related to the management of post-consumer plastics is the emission of VOCs, among which can be found compounds harmful to humans as well as the various elements of the environment. The emissions can be attributed not only to the chemical composition of virgin polymer material but also to the decomposition occurring during reprocessing, especially considering such a processing method as rotational molding, which implicates elongated subjecting of material to elevated temperatures [96,97]. The results mentioned above related to the changes in PLA molecular weight during the proposed recycling process point to the fragmentation of macromolecules, even despite the introduction of CEs, which may yield the emission of VOCs. Therefore, Figure 11 presents the total amount of VOCs (TVOC) emitted to the gaseous phase from analyzed micropellets and rotomolded parts.

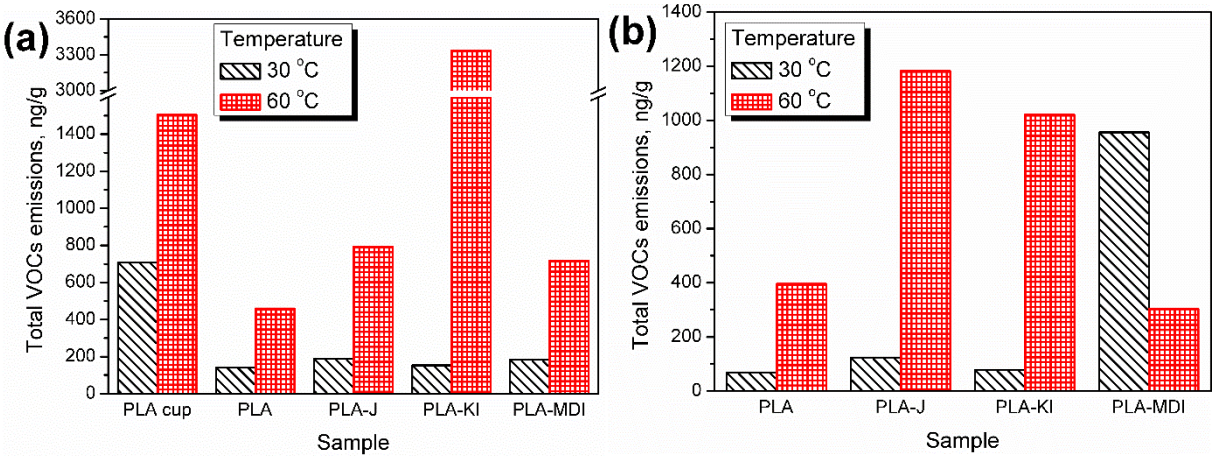

Fig. 11. The total amount of VOCs (TVOC) emitted to the gaseous phase from investigated micropellets (a) and rotomolded (b) parts.

It can be seen that at 30 °C, all of the prepared micropellets are characterized by a similar level of VOCs emissions in the range of 140-190 ng/g. The only exception is the ground PLA cup,

whose assessed TVOC parameter exceed 700 ng/g. Such an effect can be attributed to the disposable character of PLA cups, which implicates the simple composition and excludes the need for the stabilization of material, which is not subjected to the demanding conditions during its life cycle [98]. Increasing the samples conditioning temperature to 60 °C enhanced the VOCs emissions and revealed significant differences between particular samples. Higher emissions' level is attributed to the increase in vapor pressure of particular compounds. The lowest level of VOCs emissions was noted for unmodified PLA – around 460 ng/g. Similar to the 30 °C, emissions at 60 ºC for PLA cup were characterized by significantly higher emissions than PLA micropellets. The introduction of J and MDI chain extenders elevated emissions' levels to 700-800 ng/g, while the application of KI caused seven-fold increase in VOCs emissions to 3335 ng/g. These effects may be attributed to the partial decomposition of chain extenders at processing temperature (190 °C), as well as the imperfect bonding with the PLA matrix. Figure 11b provides information about the numerical values of TVOCs parameter obtained for rotomolded parts. Clearly, the modification of PLA with selected CEs yielded increased VOCs emissions from studied rotomolded parts, which are attributed to the emissions from the modifiers themselves and not from an inefficient action of selected modifiers.

Figure S2~~12~~ shows the detailed information about the emission levels of representatives of aliphatic and aromatic hydrocarbons emitted form investigated samples. Compounds have been selected for more detailed investigation due to the frequency of their occurrence among the VOCs emitted by polymeric materials and the hazards they pose to human health and the various elements of the environment [53,99,100]. In the described case, most emitted hydrocarbons were aromatics. Their presence in a gaseous phase can be associated with their common use as solvents in the plastics industry and with the decomposition of the modified PLA materials. The emission level of aromatics is noticeably higher for PLA-containing CEs, which is related to the chemical structure of applied modifiers. They all contain aromatic rings in their structure, which may lead to the emission of aromatics to the gaseous phase due to the decomposition induced by shear forces during grinding, as well as prolonged exposure to the oxidative conditions at elevated temperatures during rotational molding. The emissions are significantly higher for rotomolded parts, which confirms the decomposition of PLA during rotational molding suggested by other analyses.

Table ~~7~~S1 presents the list of VOCs, which were detected and identified in gaseous phase during the analysis of PLA cups, micropellets, and rotomolded parts. It can be seen that the list of VOCs includes various groups of the compound like aromatic, aliphatic and cyclic hydrocarbons, alcohols, aldehydes, ketones and others. However, most compounds were detected only for modified samples; therefore, it can be presumed that they originated from applied chain extenders. Among the VOCs emitted from unmodified PLA, either in the form of a cup, micropellet, or rotomolded part, can be found mainly benzene, 1,3-di-*tert*-butylbenzene, aliphatic hydrocarbons, numerous aldehydes and ketones, and acetic acid. Such observations are in-line with the literature data; however, it must be indicated that they referred to the emissions during 3D printing, so the temperature of emission was substantially higher [101–104]. Modification of PLA with chain extenders noticeably limited the emissions of multiple VOCs, mainly aldehydes, from micropellets. Such an effect may point to their high efficiency and binding capability attributed to the presence of functional groups able to attract numerous compounds. Emissions of aldehydes were also reduced after the rotational molding process,

which could also be attributed to the above-mentioned reactions, as well as their oxidation and decomposition at highly-demanding oxidative conditions. Processing of micropellets also yielded the emission of numerous hydrocarbons, not detected for micropellets, which can be associated with the chain scission decreasing the PLA molecular weight occurring during rotational molding. In the case of KI-modified parts, the nitrogen-containing compounds were detected – ligustrazine, 2,6-diisopropylphenyl isocyanate and 2,6-diisopropylaniline, pointing to the partial decomposition of its structure during rotational molding. Interestingly, these compounds have not been detected for PLA-MDI materials, which is related to their superior thermal stability, as indicated by TGA results.

Table ~~7~~S1 also provides codes and pictograms according to NFPA 704: Standard System for the Identification of the Hazards of Materials for Emergency Response and Globally Harmonized System (GHS) of Classification and Labelling of Chemicals (commonly used for the classification of chemicals by the risk they pose towards human health and safety) [105,106]. They provide information essential for assessing the threats posed by particular chemicals. The NFPA system is known as the "safety square" and describes the instability, health and flammability threats of chemical compounds on a scale from 0 to 4. The GHS system uses pictograms and hazard statements, which summarize the physical, health, and environmental properties and threats of materials. It can be seen that numerous VOCs emitted by the analyzed materials are categorized as flammable materials, which is mainly attributed to their flashpoint. However, applied modifications do not show any straightforward influence on the emissions of flammable VOCs. Considering the health hazards, 2,6-diisopropylphenyl isocyanate should be treated as the most dangerous compound among detected VOCs. It was emitted from PLA-KI micropellets and rotomolded parts. Severe hazards may also be related to limonene, tridecane, and acetic acid. The last compound is emitted from all analyzed materials, and it is a typical effect for PLA, according to literature reports [101]. Tridecane emissions were attributed to the lowering of PLA molecular weight and were noted for all modified rotomolded parts. Limonene, one of the most abundant pollutants, was detected for PLA-KI and PLA-MDI materials, which may be associated with its broad industrial use, e.g., as solvent [107]. Therefore, considering the VOCs emissions, analyzed in a quantitative and qualitative manner, KI poses as the least beneficial chain extender for PLA in terms of the safety of human health and life and the environment.

4. Conclusions

The use of chain extenders to modify waste PLA allows for its valorization and processing in the rotational molding process. The possibilities of using three different chain extenders affecting the polymer matrix differently were verified, and their effectiveness in harsh processing conditions, as the ones occurring in rotomolding, was assessed by carrying out a structurally correlated analysis of the properties and quality of the final products. The research was supplemented with a critical analysis of VOC migration, focused on the safety of using products made of modified PLA in terms of human health.

The images from 3D computed tomography show that the addition of poly(styrene-acrylic-co-methacrylate glycidyl) copolymer (J) and bis(2,6-diisopropylphenyl) carbodiimide (KI) introduced at 0.3 and 2% w/w loadings, respectively, allowing for a significant improvement in the structure of the final products. At the same time, unsatisfactory effects of the influence of

4,4'-methylenediphenyl diisocyanate (MDI) on the structure of PLA products were noted, for which a significant number of structural defects in the form of pores and inhomogeneities in the wall thickness were noted, as also happening for unmodified PLA. The increased viscosity and lower stabilization provided by using J and MDI explain the lower mechanical properties compared to KI-PLA, which provided the best results. The spectroscopic evaluation did not allow for the observation of significant changes in the base polymer structure, mainly due to the low ratio of additives used. Thermal assays demonstrated better performance for the modified materials than for the raw PLA; in any case, all materials showed enough thermal stability for the rotational molding processing.

The introduction of the three additives increased the molecular weight of PLA, which translated into changes in thermal properties and polymer structure. A 3D branched structure with cross-linking was obtained for J and MDI. Conversely, KI did not cause significant changes in the PLA structure, only acting against thermooxidative or hydrolytic degradation occurring during rotational molding and leading to stable behavior during the subsequent processing stages.

Despite degradation phenomena and changes in molecular weight, no significant increase in crystallinity occurs for the rotomolded samples. The glass transition temperatures from DMA for all modified materials resulted in higher values than for unmodified PLA, while those obtained from DSC were not significantly different. Furthermore, the maxima of α-relaxation curves were characterized by higher values of tan δ for PLA-KI and PLA-J, which may be related to the increased ductility of the materials arising from the modification of the PLA structure.

The assessment of mechanical properties confirmed the need to use chain extenders to recycle PLA by rotational molding; otherwise, the obtained parts are highly porous and provide low mechanical properties. The proposed modifiers allow obtaining parts with mechanical properties similar to those of the original material, KI providing an outstanding impact strength and toughness, increased by 8 and 10 regarding the unmodified PLA, respectively. Only PLA-KI shows similar molecular weight and rheological behavior before and after the processing, efficiently reducing the effects of thermooxidative and hydrolytic degradation reactions during the long cycle time of the rotational molding process. Thus, bis(2,6-diisopropylphenyl) carbodiimide is considered the most efficient modifier for PLA recycling, at least for rotationally molded products.

References

[1] Crawford RJ, Throne J. Rotational Molding Technology. New York: William Andrew Publishing; 2001.

[2] Głogowska K, Pączkowski P, Samujło B. Study on the Properties and Structure of Rotationally Moulded Linear Low-Density Polyethylene Filled with Quartz Flour. Materials (Basel) 2022;15:2154. https://doi.org/10.3390/ma15062154.

[3] Song SS, Nagy T, White JL. A Basic Study of Applicability of Regrind Polyethylene in Rotational Molding. Int Polym Process 1992;7:274–82. https://doi.org/10.3139/217.920274.

[4] Chaisrichawla S, Dangtungee R. The Usage of Recycled Material in Rotational

Molding Process for Production of Septic Tank. Mater Sci Forum 2018;936:151–8. https://doi.org/10.4028/www.scientific.net/MSF.936.151.
[5] Arribasplata-Seguin A, Quispe-Dominguez R, Tupia-Anticona W, Acosta-Sullcahuamán J. Rotational molding parameters of wood-plastic composite materials made of recycled high density polyethylene and wood particles. Compos Part B Eng 2021;217:108876. https://doi.org/10.1016/j.compositesb.2021.108876.
[6] Dou Y, Rodrigue D. Morphological, thermal and mechanical properties of recycled HDPE foams via rotational molding. J Cell Plast 2022;58:305–23. https://doi.org/10.1177/0021955X211013793.
[7] Suárez L, Ortega Z, Romero F, Paz R, Marrero MD. Influence of Giant Reed Fibers on Mechanical, Thermal, and Disintegration Behavior of Rotomolded PLA and PE Composites. J Polym Environ 2022. https://doi.org/10.1007/s10924-022-02542-x.
[8] Robledo-Ortíz JR, González-López ME, Rodrigue D, Gutiérrez-Ruiz JF, Prezas-Lara F, Pérez-Fonseca AA. Improving the Compatibility and Mechanical Properties of Natural Fibers/Green Polyethylene Biocomposites Produced by Rotational Molding. J Polym Environ 2020;28:1040–9. https://doi.org/10.1007/s10924-020-01667-1.
[9] Ortega Z, Romero F, Paz R, Suárez L, Benítez AN, Marrero MD. Valorization of Invasive Plants from Macaronesia as Filler Materials in the Production of Natural Fiber Composites by Rotational Molding. Polymers (Basel) 2021;13:2220. https://doi.org/10.3390/polym13132220.
[10] Díaz S, Ortega Z, McCourt M, Kearns MP, Benítez AN. Recycling of polymeric fraction of cable waste by rotational moulding. Waste Manag 2018;76:199–206. https://doi.org/10.1016/j.wasman.2018.03.020.
[11] Barczewski M, Hejna A, Aniśko J, Andrzejewski J, Piasecki A, Mysiukiewicz O, et al. Rotational molding of polylactide (PLA) composites filled with copper slag as a waste filler from metallurgical industry. Polym Test 2022;106:107449. https://doi.org/10.1016/j.polymertesting.2021.107449.
[12] Cosate de Andrade MF, Souza PMS, Cavalett O, Morales AR. Life Cycle Assessment of Poly(Lactic Acid) (PLA): Comparison Between Chemical Recycling, Mechanical Recycling and Composting. J Polym Environ 2016;24:372–84. https://doi.org/10.1007/s10924-016-0787-2.
[13] Briassoulis D, Pikasi A, Hiskakis M. Recirculation potential of post-consumer /industrial bio-based plastics through mechanical recycling - Techno-economic sustainability criteria and indicators. Polym Degrad Stab 2021;183:109217. https://doi.org/10.1016/j.polymdegradstab.2020.109217.
[14] Badia JD, Ribes-Greus A. Mechanical recycling of polylactide, upgrading trends and combination of valorization techniques. Eur Polym J 2016;84:22–39. https://doi.org/10.1016/j.eurpolymj.2016.09.005.
[15] Żenkiewicz M, Richert J, Rytlewski P, Moraczewski K, Stepczyńska M, Karasiewicz T. Characterisation of multi-extruded poly(lactic acid). Polym Test 2009;28:412–8. https://doi.org/10.1016/j.polymertesting.2009.01.012.
[16] Badia JD, Strömberg E, Karlsson S, Ribes-Greus A. Material valorisation of amorphous polylactide. Influence of thermo-mechanical degradation on the morphology, segmental dynamics, thermal and mechanical performance. Polym Degrad Stab 2012;97:670–8. https://doi.org/10.1016/j.polymdegradstab.2011.12.019.
[17] Aldhafeeri T, Alotaibi M, Barry CF. Impact of Melt Processing Conditions on the Degradation of Polylactic Acid. Polymers (Basel) 2022;14:2790. https://doi.org/10.3390/polym14142790.
[18] Beltrán FR, Lorenzo V, Acosta J, de la Orden MU, Martínez Urreaga J. Effect of simulated mechanical recycling processes on the structure and properties of poly(lactic

acid). J Environ Manage 2018;216:25–31. https://doi.org/10.1016/j.jenvman.2017.05.020.
[19] Beltrán FR, Lorenzo V, de la Orden MU, Martínez-Urreaga J. Effect of different mechanical recycling processes on the hydrolytic degradation of poly(l-lactic acid). Polym Degrad Stab 2016;133:339–48. https://doi.org/10.1016/j.polymdegradstab.2016.09.018.
[20] Cuadri AA, Martín-Alfonso JE. Thermal, thermo-oxidative and thermomechanical degradation of PLA: A comparative study based on rheological, chemical and thermal properties. Polym Degrad Stab 2018;150:37–45. https://doi.org/10.1016/j.polymdegradstab.2018.02.011.
[21] Aniśko J, Barczewski M, Mietliński P, Piasecki A, Szulc J. Valorization of disposable polylactide (PLA) cups by rotational molding technology: The influence of pre-processing grinding and thermal treatment. Polym Test 2022;107:107481. https://doi.org/10.1016/j.polymertesting.2022.107481.
[22] Cosate de Andrade MF, Fonseca G, Morales AR, Mei LHI. Mechanical recycling simulation of polylactide using a chain extender. Adv Polym Technol 2018;37:2053–60. https://doi.org/10.1002/adv.21863.
[23] Södergård A, Stolt M. Properties of lactic acid based polymers and their correlation with composition. Prog Polym Sci 2002;27:1123–63. https://doi.org/10.1016/S0079-6700(02)00012-6.
[24] Mousavi Z, Heuzey M, Randall J, Carreau PJ. Enhanced properties of polylactide/polyamide 11 blends by reactive compatibilization. Can J Chem Eng 2022;100:2475–90. https://doi.org/10.1002/cjce.24414.
[25] Shin BY, Han DH. Viscoelastic properties of PLA/PCL blends compatibilized with different methods. Korea-Australia Rheol J 2017;29:295–302. https://doi.org/10.1007/s13367-017-0029-8.
[26] Rasselet D, Caro-Bretelle A-S, Taguet A, Lopez-Cuesta J-M. Reactive Compatibilization of PLA/PA11 Blends and Their Application in Additive Manufacturing. Materials (Basel) 2019;12:485. https://doi.org/10.3390/ma12030485.
[27] Andrzejewski J, Nowakowski M. Development of Toughened Flax Fiber Reinforced Composites. Modification of Poly(lactic acid)/Poly(butylene adipate-co-terephthalate) Blends by Reactive Extrusion Process. Materials (Basel) 2021;14:1523. https://doi.org/10.3390/ma14061523.
[28] Andrzejewski J, Skórczewska K, Kloziński A. Improving the Toughness and Thermal Resistance of Polyoxymethylene/Poly(lactic acid) Blends: Evaluation of Structure–Properties Correlation for Reactive Processing. Polymers (Basel) 2020;12:307. https://doi.org/10.3390/polym12020307.
[29] Meng Q, Heuzey M-C, Carreau PJ. Control of thermal degradation of polylactide/clay nanocomposites during melt processing by chain extension reaction. Polym Degrad Stab 2012;97:2010–20. https://doi.org/10.1016/j.polymdegradstab.2012.01.030.
[30] Limsukon W, Auras R, Selke S. Hydrolytic degradation and lifetime prediction of poly(lactic acid) modified with a multifunctional epoxy-based chain extender. Polym Test 2019;80:106108. https://doi.org/10.1016/j.polymertesting.2019.106108.
[31] Najafi N, Heuzey MC, Carreau PJ, Wood-Adams PM. Control of thermal degradation of polylactide (PLA)-clay nanocomposites using chain extenders. Polym Degrad Stab 2012;97:554–65. https://doi.org/10.1016/j.polymdegradstab.2012.01.016.
[32] Kahraman Y, Özdemir B, Kılıç V, Goksu YA, Nofar M. Super toughened and highly ductile PLA/TPU blend systems by in situ reactive interfacial compatibilization using multifunctional epoxy-based chain extender. J Appl Polym Sci 2021;138:50457. https://doi.org/10.1002/app.50457.

[33] Yang L, Chen X, Jing X. Stabilization of poly(lactic acid) by polycarbodiimide. Polym Degrad Stab 2008;93:1923–9. https://doi.org/10.1016/j.polymdegradstab.2008.06.016.
[34] Zhong W, Ge J, Gu Z, Li W, Chen X, Zang Y, et al. Study on biodegradable polymer materials based on poly(lactic acid). I. Chain extending of low molecular weight poly(lactic acid) with methylenediphenyl diisocyanate. J Appl Polym Sci 1999;74:2546–51. https://doi.org/10.1002/(SICI)1097-4628(19991205)74:10<2546::AID-APP24>3.0.CO;2-Z.
[35] Hao Y, Li Y, Liu Z, Yan X, Tong Y, Zhang H. Thermal, Mechanical and Rheological Properties of Poly(lactic acid) Chain Extended with Polyaryl Polymethylene Isocyanate. Fibers Polym 2019;20:1766–73. https://doi.org/10.1007/s12221-019-8579-7.
[36] Gu S, Yang M, Yu T, Ren T, Ren J. Synthesis and characterization of biodegradable lactic acid-based polymers by chain extension. Polym Int 2008;57:982–6. https://doi.org/10.1002/pi.2435.
[37] Meng X, Shi G, Chen W, Wu C, Xin Z, Han T, et al. Structure effect of phosphite on the chain extension in PLA. Polym Degrad Stab 2015;120:283–9. https://doi.org/10.1016/j.polymdegradstab.2015.07.019.
[38] Coltelli M-B, Bertolini A, Aliotta L, Gigante V, Vannozzi A, Lazzeri A. Chain Extension of Poly(Lactic Acid) (PLA)–Based Blends and Composites Containing Bran with Biobased Compounds for Controlling Their Processability and Recyclability. Polymers (Basel) 2021;13:3050. https://doi.org/10.3390/polym13183050.
[39] Panariello L, Coltelli M-B, Vannozzi A, Bonacchi D, Aliotta L, Lazzeri A. Fully Biobased Reactive Extrusion of Biocomposites Based on PLA Blends and Hazelnut Shell Powders (HSP). Chemistry (Easton) 2021;3:1464–80. https://doi.org/10.3390/chemistry3040104.
[40] Quiles-Carrillo L, Duart S, Montanes N, Torres-Giner S, Balart R. Enhancement of the mechanical and thermal properties of injection-molded polylactide parts by the addition of acrylated epoxidized soybean oil. Mater Des 2018;140:54–63. https://doi.org/10.1016/j.matdes.2017.11.031.
[41] Inata H, Matsumura S. Chain extenders for polyesters. I. Addition-type chain extenders reactive with carboxyl end groups of polyesters. J Appl Polym Sci 1985;30:3325–37. https://doi.org/10.1002/app.1985.070300815.
[42] Sambha'a EL, Lallam A, Jada A. Effect of Hydrothermal Polylactic Acid Degradation on Polymer Molecular Weight and Surface Properties. J Polym Environ 2010;18:532–8. https://doi.org/10.1007/s10924-010-0251-7.
[43] Spatorico AL, Coulter B. Molecular weight determinations by gel-permeation chromatography and viscometry. J Polym Sci Part A-2 Polym Phys 1973;11:1139–50. https://doi.org/10.1002/pol.1973.180110608.
[44] Schindler A, Harper D. Polylactide. II. Viscosity–molecular weight relationships and unperturbed chain dimensions. J Polym Sci Polym Chem Ed 1979;17:2593–9. https://doi.org/10.1002/pol.1979.170170831.
[45] International Commission on Illumination. Recommendations on uniform color spaces, color-difference equations, psychometric color terms. C.I.E.; 1978.
[46] Bociaga E, Trzaskalska M. Influence of polymer processing parameters and coloring agents on gloss and color of acrylonitrile-butadiene-styrene terpolymer moldings. Polimery 2016;61:544–50. https://doi.org/10.14314/polimery.2016.544.
[47] Garlotta D. A Literature Review of Poly (Lactic Acid) A Literature Review of Poly (Lactic Acid). J Polym Environ 2019;9:63–84.
[48] Brostow W, Hagg Lobland HE, Khoja S. Brittleness and toughness of polymers and other materials. Mater Lett 2015;159:478–80.

https://doi.org/https://doi.org/10.1016/j.matlet.2015.07.047.
[49] Marć M, Namieśnik J, Zabiegała B. The miniaturised emission chamber system and home-made passive flux sampler studies of monoaromatic hydrocarbons emissions from selected commercially-available floor coverings. Build Environ 2017;123:1–13. https://doi.org/10.1016/j.buildenv.2017.06.035.
[50] Schripp T, Nachtwey B, Toelke J, Salthammer T, Uhde E, Wensing M, et al. A microscale device for measuring emissions from materials for indoor use. Anal Bioanal Chem 2007;387:1907–19. https://doi.org/10.1007/s00216-006-1057-2.
[51] Marć M, Tsakovski S, Tobiszewski M. Emissions and toxic units of solvent, monomer and additive residues released to gaseous phase from latex balloons. Environ Res 2021;195:110700. https://doi.org/10.1016/j.envres.2020.110700.
[52] Zabiegała B, Sărbu C, Urbanowicz M, Namieśnik J. A Comparative Study of the Performance of Passive Samplers. J Air Waste Manage Assoc 2011;61:260–8. https://doi.org/10.3155/1047-3289.61.3.260.
[53] Wojnowski W, Marć M, Kalinowska K, Kosmela P, Zabiegała B. Emission Profiles of Volatiles during 3D Printing with ABS, ASA, Nylon, and PETG Polymer Filaments. Molecules 2022;27:3814. https://doi.org/10.3390/molecules27123814.
[54] Li P, Zhang W, Kong M, Lv Y, Huang Y, Yang Q, et al. Ultrahigh performance polylactide achieved by the design of molecular structure. Mater Des 2021;206:109779. https://doi.org/10.1016/j.matdes.2021.109779.
[55] Zeng J-B, Li Y-D, Zhu Q-Y, Yang K-K, Wang X-L, Wang Y-Z. A novel biodegradable multiblock poly(ester urethane) containing poly(l-lactic acid) and poly(butylene succinate) blocks. Polymer (Guildf) 2009;50:1178–86. https://doi.org/10.1016/j.polymer.2009.01.001.
[56] Liu W, Li H, Wang X, Du Z, Zhang C. Effect of Chain Extension on the Rheological Property and Thermal Behaviour of Poly(lactic acid) Foams. Cell Polym 2013;32:343–68. https://doi.org/10.1177/026248931303200602.
[57] Laske S, Ziegler W, Kainer M, Wuerfel J, Holzer C. Enhancing the temperature stability of PLA by compounding strategies. Polym Eng Sci 2015;55:2849–58. https://doi.org/10.1002/pen.24176.
[58] Taib N-AAB, Rahman MR, Huda D, Kuok KK, Hamdan S, Bakri MK Bin, et al. A review on poly lactic acid (PLA) as a biodegradable polymer. Polym Bull 2022. https://doi.org/10.1007/s00289-022-04160-y.
[59] Khankrua R, Pivsa-Art S, Hiroyuki H, Suttiruengwong S. Effect of chain extenders on thermal and mechanical properties of poly(lactic acid) at high processing temperatures: Potential application in PLA/Polyamide 6 blend. Polym Degrad Stab 2014;108:232–40. https://doi.org/10.1016/j.polymdegradstab.2014.04.019.
[60] Yang S, Wu Z-H, Yang W, Yang M-B. Thermal and mechanical properties of chemical crosslinked polylactide (PLA). Polym Test 2008;27:957–63. https://doi.org/10.1016/j.polymertesting.2008.08.009.
[61] Kopinke F-D, Mackenzie K. Mechanistic aspects of the thermal degradation of poly(lactic acid) and poly(β-hydroxybutyric acid). J Anal Appl Pyrolysis 1997;40–41:43–53. https://doi.org/10.1016/S0165-2370(97)00022-3.
[62] Gwon J-G, Cho H-J, Chun S-J, Lee S, Wu Q, Li M-C, et al. Mechanical and thermal properties of toluene diisocyanate-modified cellulose nanocrystal nanocomposites using semi-crystalline poly(lactic acid) as a base matrix. RSC Adv 2016;6:73879–86. https://doi.org/10.1039/C6RA10993D.
[63] Stepczynska M. Effect of UV-VIS radiation on the thermomechanical properties and structure of dyed PLA film. Polimery 2015;60:385–90. https://doi.org/10.14314/polimery.2015.385.

[64] H. Hoidy W, B. Ahmad M, Jaffar Al- EA, Bt Ibrahim NA. Preparation and Characterization of Polylactic Acid/Polycaprolactone Clay Nanocomposites. J Appl Sci 2010;10:97–106. https://doi.org/10.3923/jas.2010.97.106.
[65] Singla P, Mehta R, Berek D, Upadhyay SN. Microwave Assisted Synthesis of Poly(lactic acid) and its Characterization using Size Exclusion Chromatography. J Macromol Sci Part A 2012;49:963–70. https://doi.org/10.1080/10601325.2012.722858.
[66] Auras R, Harte B, Selke S. An Overview of Polylactides as Packaging Materials. Macromol Biosci 2004;4:835–64. https://doi.org/10.1002/mabi.200400043.
[67] Ucpinar Durmaz B, Atılgan MG, Aytac A. Evaluation of the morphological, rheological, dynamic mechanical and mechanical characteristics of compatibilized graphene oxide/poly(ethylene terephthalate)/poly(butylene terephthalate) nanocomposites. Polym Compos 2021;42:6941–51. https://doi.org/10.1002/pc.26352.
[68] Fug F, Nies C, Possart W. in situ FTIR study of adhesive interactions of 4,4′-methylene diphenyl diisocyanate and native metals. Int J Adhes Adhes 2014;52:66–76. https://doi.org/10.1016/j.ijadhadh.2014.04.004.
[69] Arunkumar T, Ramachandran S. Surface coating and characterisation of polyurea for liquid storage. Int J Ambient Energy 2017;38:781–7. https://doi.org/10.1080/01430750.2016.1222966.
[70] Grigora M-E, Terzopoulou Z, Tsongas K, Klonos P, Kalafatakis N, Bikiaris DN, et al. Influence of Reactive Chain Extension on the Properties of 3D Printed Poly(Lactic Acid) Constructs. Polymers (Basel) 2021;13:1381. https://doi.org/10.3390/polym13091381.
[71] Okrasa M, Leszczyńska M, Sałasińska K, Szczepkowski L, Kozikowski P, Majchrzycka K, et al. Viscoelastic Polyurethane Foams for Use in Seals of Respiratory Protective Devices. Materials (Basel) 2021;14:1600. https://doi.org/10.3390/ma14071600.
[72] Masek A. Flavonoids as Natural Stabilizers and Color Indicators of Ageing for Polymeric Materials. Polymers (Basel) 2015;7:1125–44. https://doi.org/10.3390/polym7061125.
[73] Allen NS, Edge M, Hussain S. Perspectives on yellowing in the degradation of polymer materials: inter-relationship of structure, mechanisms and modes of stabilisation. Polym Degrad Stab 2022;201:109977. https://doi.org/10.1016/j.polymdegradstab.2022.109977.
[74] Safandowska M, Rozanski A, Galeski A. Plasticization of Polylactide after Solidification: An Effectiveness and Utilization for Correct Interpretation of Thermal Properties. Polymers (Basel) 2020;12:561. https://doi.org/10.3390/polym12030561.
[75] Di Lorenzo ML. Calorimetric analysis of the multiple melting behavior of poly(L-lactic acid). J Appl Polym Sci 2006;100:3145–51. https://doi.org/10.1002/app.23136.
[76] Androsch R, Schick C, Di Lorenzo ML. Melting of Conformationally Disordered Crystals (α′-Phase) of Poly(<scp>l</scp> -lactic acid). Macromol Chem Phys 2014;215:1134–9. https://doi.org/10.1002/macp.201400126.
[77] Fukushima K, Tabuani D, Dottori M, Armentano I, Kenny JM, Camino G. Effect of temperature and nanoparticle type on hydrolytic degradation of poly(lactic acid) nanocomposites. Polym Degrad Stab 2011;96:2120–9. https://doi.org/10.1016/j.polymdegradstab.2011.09.018.
[78] Wu F, Misra M, Mohanty AK. Studies on why the heat deflection temperature of polylactide bioplastic cannot be improved by overcrosslinking. Polym Cryst 2019;2. https://doi.org/10.1002/pcr2.10088.
[79] Ogila KO, Shao M, Yang W, Tan J. Rotational molding: A review of the models and materials. Express Polym Lett 2017;11:778–98.

https://doi.org/10.3144/expresspolymlett.2017.75.
[80] Qian Z, McKenna GB. Expanding the application of the van Gurp-Palmen plot: New insights into polymer melt rheology. Polymer (Guildf) 2018;155:208–17. https://doi.org/10.1016/j.polymer.2018.09.036.
[81] Cailloux J, Santana OO, Franco-Urquiza E, Bou JJ, Carrasco F, Gamez-Perez J, et al. Sheets of branched poly(lactic acid) obtained by one step reactive extrusion calendering process: Melt rheology analysis. Express Polym Lett 2013;7:304–18. https://doi.org/10.3144/expresspolymlett.2013.27.
[82] Ferry JD. Viscoelastic Properties of Polymers. 3rd Editio. New York: Wiley; 1980.
[83] Barczewski M, Mysiukiewicz O. Rheological and Processing Properties of Poly(lactic acid) Composites Filled with Ground Chestnut Shell. Polym Korea 2018;42:267–74. https://doi.org/10.7317/pk.2018.42.2.267.
[84] Kashi S, Gupta RK, Baum T, Kao N, Bhattacharya SN. Phase transition and anomalous rheological behaviour of polylactide/graphene nanocomposites. Compos Part B Eng 2018;135:25–34. https://doi.org/10.1016/j.compositesb.2017.10.002.
[85] Fazelinejad S, Åkesson D, Skrifvars M. Repeated Mechanical Recycling of Polylactic Acid Filled with Chalk. Prog Rubber, Plast Recycl Technol 2017;33:1–16. https://doi.org/10.1177/147776061703300101.
[86] Gupta N, Ramkumar P, Sangani V. An approach toward augmenting materials, additives, processability and parameterization in rotational molding: a review. Mater Manuf Process 2020;35:1539–56. https://doi.org/10.1080/10426914.2020.1779934.
[87] Baimark Y, Cheerarot O. Effect of Chain Extension on Thermal Stability Behaviors of Polylactide Bioplastics. Orient J Chem 2015;31:635–41.
[88] Kontopoulou M, Vlachopoulos J. Bubble dissolution in molten polymers and its role in rotational molding. Polym Eng Sci 1999;39:1189–98. https://doi.org/10.1002/pen.11505.
[89] Notta-Cuvier D, Odent J, Delille R, Murariu M, Lauro F, Raquez JM, et al. Tailoring polylactide (PLA) properties for automotive applications: Effect of addition of designed additives on main mechanical properties. Polym Test 2014;36:1–9. https://doi.org/10.1016/j.polymertesting.2014.03.007.
[90] Aniśko J, Barczewski M. Polylactide: from Synthesis and Modification to Final Properties. Adv Sci Technol Res J 2021;15:9–29. https://doi.org/10.12913/22998624/137960.
[91] Zhao X, Hu H, Wang X, Yu X, Zhou W, Peng S. Super tough poly(lactic acid) blends: a comprehensive review. RSC Adv 2020;10:13316–68. https://doi.org/10.1039/D0RA01801E.
[92] Vetter L, Werner J, Wolf M, Hertle S, Drummer D. Influence of vacuum on the porosity and mechanical properties in rotational molding. Polym Eng Sci 2019;59:1544–51. https://doi.org/10.1002/pen.25152.
[93] Crawford RJ, Spence AG, Cramez MC, Oliveira MJ. Mould pressure control in rotational moulding. Proc Inst Mech Eng Part B J Eng Manuf 2004;218:1683–93. https://doi.org/10.1177/095440540421801204.
[94] Ortiz-Barajas DL, Arévalo-Prada JA, Fenollar O, Rueda-Ordóñez YJ, Torres-Giner S. Torrefaction of Coffee Husk Flour for the Development of Injection-Molded Green Composite Pieces of Polylactide with High Sustainability. Appl Sci 2020;10:6468. https://doi.org/10.3390/app10186468.
[95] Deng S, Hou M, Ye L. Temperature-dependent elastic moduli of epoxies measured by DMA and their correlations to mechanical testing data. Polym Test 2007;26:803–13. https://doi.org/10.1016/j.polymertesting.2007.05.003.
[96] Lattuati-Derieux A, Egasse C, Thao-Heu S, Balcar N, Barabant G, Lavédrine B. What

do plastics emit? HS-SPME-GC/MS analyses of new standard plastics and plastic objects in museum collections. J Cult Herit 2013;14:238–47. https://doi.org/10.1016/j.culher.2012.06.005.
[97] Hahladakis JN, Velis CA, Weber R, Iacovidou E, Purnell P. An overview of chemical additives present in plastics: Migration, release, fate and environmental impact during their use, disposal and recycling. J Hazard Mater 2018;344:179–99. https://doi.org/10.1016/j.jhazmat.2017.10.014.
[98] Jamshidian M, Tehrany EA, Imran M, Jacquot M, Desobry S. Poly-Lactic Acid: Production, Applications, Nanocomposites, and Release Studies. Compr Rev Food Sci Food Saf 2010;9:552–71. https://doi.org/10.1111/j.1541-4337.2010.00126.x.
[99] Marć M, Rutkowska M, Hejna A, Barczewski M. Biocomposites from recycled resources as candidates for laboratory reference material to validate analytical tools used in organic compounds emissions investigation. Build Environ 2022;219:109259. https://doi.org/10.1016/j.buildenv.2022.109259.
[100] Śmiełowska M, Marć M, Zabiegała B. Small Polymeric Toys Placed in Child-Dedicated Chocolate Food Products—Do They Contain Harmful Chemicals? Examination of Quality by Example of Selected VOCs and SVOCs. Expo Heal 2022;14:203–16. https://doi.org/10.1007/s12403-021-00428-2.
[101] Byrley P, Geer Wallace MA, Boyes WK, Rogers K. Particle and volatile organic compound emissions from a 3D printer filament extruder. Sci Total Environ 2020;736:139604. https://doi.org/10.1016/j.scitotenv.2020.139604.
[102] Davis AY, Zhang Q, Wong JPS, Weber RJ, Black MS. Characterization of volatile organic compound emissions from consumer level material extrusion 3D printers. Build Environ 2019;160:106209. https://doi.org/10.1016/j.buildenv.2019.106209.
[103] Azimi P, Zhao D, Pouzet C, Crain NE, Stephens B. Emissions of Ultrafine Particles and Volatile Organic Compounds from Commercially Available Desktop Three-Dimensional Printers with Multiple Filaments. Environ Sci Technol 2016;50:1260–8. https://doi.org/10.1021/acs.est.5b04983.
[104] Wojnowski W, Kalinowska K, Majchrzak T, Zabiegała B. Real-time monitoring of the emission of volatile organic compounds from polylactide 3D printing filaments. Sci Total Environ 2022;805:150181. https://doi.org/10.1016/j.scitotenv.2021.150181.
[105] European Parliament and the Council (2008) Regulation (EC) No 1272/2008 of the European Parliament and of the Council of 16 December 2008 on classification, labelling and packaging of substances and mixtures, amending and repealing Directives 67/548/EEC a. 2008.
[106] NFPA (2017) NFPA 704: standard system for the identification of the hazards of materials for emergency response. 2017.
[107] Nematollahi N, Ross PA, Hoffmann AA, Kolev SD, Steinemann A. Limonene Emissions: Do Different Types Have Different Biological Effects? Int J Environ Res Public Health 2021;18:10505. https://doi.org/10.3390/ijerph181910505.